The Effect of Exposure Conditions on the Long-term Performance Evaluation of Undamaged and Damaged Wire-arc Sprayed Zinc-Aluminum Alloy Coatings

Ratna Divya Yasoda[a], Ying Huang[a*], and Xiaoning Qi[b]

[a] Department of Civil, Construction, and Environmental Engineering., North Dakota State University, Fargo, USA
Email: ratna.yasoda@ndus.edu; ying.huang@ndsu.edu
[b] Department of Coatings and Polymeric Materials, North Dakota State University, Fargo, USA
Email: xiaoning.qi@ndsu.edu.
* Corresponding author

Abstract

This study examined the influence of laboratory corrosion testing methods, specifically salt spray, and immersion tests, on the long-term performance assessment of wire-arc sprayed Zn-Al coatings. Two Zn-Al alloyed systems, Zn-15Al and Zn-Al pseudo alloy, were selected for investigation, subjecting them to 1000 hours of immersion and salt spray conditions. Electrochemical impedance spectroscopy (EIS) was used to monitor corrosion progression in both coating systems at 200-hour intervals. Post-exposure, the coatings underwent microstructural and chemical characterization, along with potentiodynamic polarization tests. Furthermore, some specimens in both coating systems were intentionally damaged and exposed to 1000 hours of salt spray and immersion testing and analyzed with scanning electron microscopy (SEM). Immersion testing yielded similar results for both coatings, while salt spray testing unveiled significant differences and highlighted the susceptibility of the Zn-15Al to salt spray in both undamaged and damaged states. The continuously refreshed salt spray electrolyte hindered stable corrosion product formation, allowing chloride penetration and increased corrosion in Zn-15Al. Conversely, the Zn-Al pseudo alloy coating formed Al $(OH)_3$, acting as a barrier against chloride penetration during salt spray and offering superior protection. In summary, salt spray testing proved more aggressive than immersion when evaluating Zn-Al coatings with high zinc content primarily relying on active dissolution for corrosion protection.

Keywords: Corrosion testing methods; Cathodic protection; Salt spray testing; Immersion testing; Corrosion mitigation.

Introduction

Thermally sprayed zinc (Zn), aluminum (Al), and Zn-Al alloy coatings are widely applied to protect steel structures from corrosion. The chloride or seawater environment is one of the most aggressive environments, causing severe corrosion in steel. Hence, these protective coatings (Zn, Al, and Zn-Al alloy) are often evaluated in different kinds of chloride environments (Ref 1,2). Laboratory electrochemical tests using synthetic seawater as an electrolyte are often employed to assess the corrosion behavior of these protective coatings in an accelerated manner. On the other hand, to evaluate the coating's long-term protection performance, either field tests or prolonged exposure tests in salt spray and immersion exposure conditions are conducted in combination with electrochemical measurements (Ref 3–6). It is worth mentioning here that the salt spray exposure conditions are aggressive and accelerated in nature and not a true representation of the real-time field exposure condition but serve as a valuable tool to assess the corrosion resistance of the coatings specifically to simulate the corrosion environment for coated steels serving under marine splash zones (Ref 7).

A few great reports investigating the long-term corrosion behavior of Zn and Al coatings via field tests are available in the literature. For example, in a study by Katayama et al. (Ref 8) the long-term atmospheric corrosion properties of the thermally sprayed Zn, Al, and Zn-Al coatings of varying thicknesses were evaluated by exposing them to the Choshi test site of Japan weathering test center for about 33 years. The coatings were analyzed using electrochemical impedance measurements and several other analytical techniques. The study provided valuable insights into the coatings' long-term behavior including the changes in the coatings' thickness, formation of corrosion products, intrusion of various aggressive ions such as chlorides and sulfates, etc. In addition, the study also indicated that pure Al and Zn-Al alloy coatings exhibited better corrosion

protection behavior compared to pure Zn coatings. Another 18-year exposure study was conducted by Kuroda et al. (Ref 9), in Japan, comparing the long-term performance of Zn, Al, and Zn-Al coatings with and without sealants in a marine environment. The results of the study revealed that the Al and Zn-Al alloy coatings of 175µm thickness maintained their excellent corrosion protection properties under severe marine conditions, whereas Zn coatings both with and without sealing started to suffer degradation in the immersed portion after 7 years of exposure. These two field tests emphasized the superior corrosion protection offered by composite or alloy coatings of Zn and Al. Later a two-year study conducted on Zn-25Al alloy and Zn-55Al-Si coatings on steel in tidal and immersion environments indicated that Zn-25Al alloy coating presented a favorable combination of uniform corrosion and pitting corrosion resistance reiterating the findings from earlier field tests (Ref 10). Similarly, another research involving exposure tests in natural environments including both seawater and freshwater environments, and laboratory conditions on thermally sprayed Zn-Al coatings revealed that the composite or alloy systems of Zn and Al outperformed the single metal systems (Ref 11). These studies reported that pure Zn coatings undergo faster dissolution while pure Al coatings tend to form localized pits whereas the alloy coatings of Zn-Al exhibit the combined cathodic and barrier actions when exposed to the corrosive environments.

While field tests on these protective coatings can provide valuable insights into their long-term behavior, they often require a significant amount of time to accurately assess the coating's behavior, which can hinder the development or improvement of coatings in a timely manner. In addition, factors such as weather, temperature, humidity, and exposure to various chemicals can vary widely, making it challenging to isolate the impact of individual variables on the coating's performance. Moreover, conducting field tests by setting up monitoring equipment, ensuring data

collection accuracy, and maintaining long-term monitoring efforts can be costly and resource-intensive. Therefore, researchers regularly employ prolonged exposure tests in salt spray or immersion exposure conditions to evaluate the performance of thermally sprayed Zn-Al coatings, owing to the several advantages provided by these test methods. The controlled conditions in salt spray and immersion exposure tests ensure consistency and reliability. In addition, the accelerated nature of the testing allows quick observations of corrosion effects and allows researchers to isolate variables to evaluate their impact. Furthermore, the increased throughput improves understanding and offers cost-effective testing.

As seen from the literature on field testing of the coatings mentioned above, it is evident that alloys of Zn and Al offer better corrosion protection to steel compared to respective single metal systems. Therefore, the performance of thermal spray coatings produced from the alloys of Zn and Al has been investigated by researchers to assess their long-term behavior using immersion exposure or salt spray exposure tests. Many such studies also involve comparing the corrosion behavior of Zn-Al alloy coatings with pure Zn and pure Al coatings. For instance, a study (Ref 12) investigated the accelerated corrosion behavior of wire-arc sprayed Zn-15Al coatings by subjecting them to a 2000-hour salt spray test and compared the performance with Zn, and Al coatings. The corrosion of the coatings was assessed as the ratio of the corroded area of the specimens which indicated that Zn-15Al coatings had a higher corrosion resistance than the Zn and Al coatings. In another research (Ref 13) the corrosion performance of a composite/alloy coating of Zn-Al after adding a rare earth element was investigated through prolonged immersion exposure. The coating was evaluated periodically investigating the changes in corrosion morphologies and electrochemical measurements. The results of the study suggested that the

coating acted as both a physical barrier and as a sacrificial anode and exhibited a superior protection performance.

In recent years, Zn-Al coatings were also produced by using individual pure metal wires of Zn and Al as feedstock wires which were then melted in the wire arc spray gun resulting in the formation of a composite coating of Zn-Al often referred to as "pseudo alloy of Zn-Al" (Ref 14). In one of the studies, the authors investigated the corrosion behavior of wire-arc sprayed Zn-15Al alloy coating produced using pre-alloyed wires as feedstock with that of Zn-15Al produced through pseudo alloying. The performance of the coatings was compared using morphological characterization and potentiodynamic polarization tests after subjecting both coatings to a 400-hour salt spray test (Ref 15). The results show that the Zn-Al pseudo alloy coating had a better corrosion resistance compared to the Zn-Al alloy coating. More recently, some studies focusing on evaluating the performance of Zn-Al pseudo alloy coatings were published. For example, in an earlier own study by authors, the corrosion behavior of Zn-15Al coating and Zn-Al pseudo alloy coating with higher aluminum content was investigated (Ref 16) during a 400-hour salt spray test. It was found that an accumulation of simonkolleite was observed in both coatings and the Zn-Al pseudo coating showed superior corrosion resistance compared with the Zn-15Al coating. The mineral simonkolleite ($Zn_5(OH)_8Cl_2 \cdot H_2O$) is a frequently found corrosion product on Zn coatings that are exposed to chloride environments. This can be attributed to the mineral's limited solubility in water at neutral pH values. As a result, simonkolleite tends to accumulate on the coating's surface, where it is detected as a stable corrosion product of Zn (Ref 17,18). Furthermore, some researchers also made efforts to investigate the underlying corrosion mechanism of Zn-Al pseudo alloy coatings by conducting prolonged immersion exposure tests and periodic electrochemical measurements on them (Ref 19). The results indicated promising long-term corrosion protection

by the pseudo alloy coating in a seawater environment through a combination of cathodic protection and barrier action.

From the above literature review, although there exists substantial work on the Zn-Al coatings, there is no consistency in the type of exposure conditions in which these coatings are being tested and no emphasis on the effect of salt spray and immersion conditions on the evaluation of the coating's long-term behavior. Although both immersion and salt spray utilize the aqueous solution of NaCl as the corrosive environment, the main difference between the two methods lies in the way the environment interacts with the coatings (Ref 20). In the salt spray test, the coating interacts with a fine layer of electrolyte, containing oxygen from the atmosphere which gets refreshed and deposited continuously on the surface of the coating. Conversely, immersion tests expose the coating surface to a stagnant bulk electrolyte in contact with the surrounding air. Research shows that this varying thickness of the electrolyte layer impacts various corrosion processes, such as the accumulation of corrosion products which affects the anodic dissolution rate, transport of oxygen that controls the cathodic process, and metal ions hydration (Ref 21,22). Multiple studies focusing on hydrophobic coatings (Ref 23), and alloys of magnesium (Ref 24,25) have shown notable disparities in the observed corrosion mechanisms and protection performance between the salt spray and immersion methods. For instance, a study conducted on anodized and post-treated aerospace aluminum alloys showed that the salt spray and immersion testing provided substantially different results for cerium-treated oxides compared to hydrothermally sealed oxides (Ref 20). However, to the best of the authors' knowledge, no such study is available focusing on the impact of different corrosion testing methods on the thermally sprayed Zn-Al coatings in the literature.

In the present work, the corrosion performance of wire-arc sprayed Zn-15Al coatings produced using a pre-alloyed wire feedstock and Zn-Al pseudo alloy coatings with an aluminum content of more than 15wt.% was compared by subjecting both coatings to prolonged salt spray and immersion conditions. This study aimed to enrich the comprehension of the consequences associated with the choice of corrosion testing methods in the evaluation and prediction of the extended durability of these highly promising Zn-Al anti-corrosive coatings. By employing the electrochemical impedance spectroscopy (EIS) technique, the corrosion protection mechanism of Zn-Al composite coatings, which predominantly relies on the synergistic effects of barrier and cathodic protection, was periodically observed and analyzed. Other characterization methods including scanning electron microscopy (SEM), energy dispersive X-ray (EDS) analysis, X-ray diffraction (XRD) study, and potentiodynamic polarization scanning (PDS) were employed on the coatings to complement the information obtained from the EIS study. Furthermore, this investigation encompassed not only the study of coatings in undamaged conditions but also the examination of their performance when damaged. To this end, the coated steel plates were intentionally subjected to simulated damage by machining artificial defects, mimicking conditions that expose the underlying substrate steel. These damaged coatings were also subjected to extended periods of salt spray and immersion exposure which allowed for the investigation of corrosion product formation on the exposed steel surface to gain insights into the protective performance of the coatings. Visual assessment, SEM imaging, and EDS mapping of elements were employed to evaluate the cathodic protection provided by the sacrificial Zn-Al coatings in the vicinity of the damaged areas.

Coating Application and Sample Preparation Protocols

This study utilized grit-blasted structural steel plates (ASTM A 36 of size 76mm x 76mm x 3.175mm) as substrates. Commercially available pre-alloyed Zn-15Al wires (1.6mm diameter) popular with the trade name TH650 were used as feedstock wires to produce Zn-15Al coating on the steel plates. On the other hand, to produce Zn-Al pseudo alloy coating, one pure Zn wire with 99.8% zinc (TH700), and one pure Al wire with 99.5% aluminum (TH600) each with a diameter of 1.6mm was used as feedstock wires on opposite sides of the wire-arc spray gun (Thermion, Poulsbo, WA, USA) equipped with a robotic arm setup for spraying. Simultaneous melting of both metal wires using this setup resulted in the formation of a Zn-Al pseudo alloy coating. All the feedstock wires were purchased from Thermion (Thermion, Poulsbo, WA, USA). The spray parameters used for the wire-arc process are presented in **Table 1**. The average thickness of the Zn-15Al coating was determined to be 300 ± 25µm, while the Zn-Al pseudo alloy coating exhibited an average thickness of 250 ± 25µm. These thickness measurements were acquired from cross-sectional micrographs of the coatings, employing Image J software. To ensure accuracy, a minimum of 15 measurements were taken from micrographs captured at four distinct locations, and these measurements were then used to calculate the coatings' average thickness. The average composition of the Zn-15Al coating closely mirrored that of the feedstock wire, comprising 79.05wt.% zinc, 17.20wt.% aluminum, and 3.75wt.% oxygen. In contrast, the Zn-Al pseudo alloy coating exhibited a composition of 58.60wt.% zinc, 37.05wt.% aluminum, and 4.35wt.% oxygen. These chemical compositions were derived as average values through EDS analysis conducted at six distinct locations on the cross-sections of both coatings, ensuring comprehensive and representative results. As previously stated, certain coated plates were intentionally subjected to artificial defects to evaluate and analyze the protective capabilities of these coatings near the damaged areas. To achieve this, a 45º chamfer mill was employed to create scribed lines in the

coating. Prior to the salt spray and immersion testing, the edges and the back of the coated plates were meticulously masked to ward off crevice corrosion initiation.

Accelerated Corrosion Testing Methods: Salt Spray and Immersion Tests

The Zn-15Al and Zn-Al pseudo alloy coatings were subjected to continuous exposure to the salt spray, as per the guidelines of ASTM B 117 (Ref 26) using a Q-fog CCT-1100 cyclic corrosion testing chamber (Q-lab corporation, Westlake, OH, USA). Additionally, the coatings designated for the immersion test were placed inside the salt spray chamber in a 1.5L beaker, which was filled with the same 5.0wt.% NaCl solution used to operate the salt spray chamber. This ensured that both the salt spray and immersion specimens experienced identical electrolyte concentration and temperature conditions. The primary difference between the salt spray exposed and immersion exposed coatings was the thickness of the electrolyte layer that the specimens were subjected to, which would provide insights into the way these coatings respond to salt spray and immersion exposure conditions. In this study, the specimens were subjected to continuous exposure under both salt spray and immersion conditions, totaling 1000 hours. This extensive duration allowed for a comprehensive assessment of their performance in each corrosive environment. It's worth noting that, at regular intervals of 200 hours, six specimens from each exposure condition were removed from the chamber. This was done to record changes in electrochemical impedance measurements with an increase in exposure duration. Importantly, these specimens were not reintroduced into the chamber to ensure that all specimens underwent uninterrupted/continuous exposure without extended breaks.

Characterization of Coatings

A comprehensive analysis was conducted to evaluate the microstructural characteristics that significantly influence the corrosion performance of the coatings. This assessment involved various factors, including the distribution of Zn and Al, as well as the elemental compositions of the coatings in their as-sprayed state. Furthermore, the thickness of the corrosion products formed, changes in the distribution of elements, the extent of oxidation, and the penetration of chloride ions were examined for both undamaged and damaged coatings after subjecting them to 1000 hours of salt spray and immersion conditions. To investigate these morphological changes in the coatings, SEM was employed. Additionally, EDS was utilized to analyze the chemical composition of the coatings and for performing elemental mapping. The SEM and EDS analyses were carried out using a JOEL JSM-6490 LV (JOEL, Peabody, MA, USA) operating at 15ke V. The imaging was performed either in secondary imaging or backscattered imaging mode. Elemental analysis was performed by a nano trace EDS detector equipped with a NORVAR light element window (Thermo Scientific, Madison, WI, USA), in conjunction with a Noran System six imaging system 202 (Thermo Scientific) in the SEM set up. The EDS instrument is calibrated to copper (Cu- Kα) 8041eV and can detect the elements from boron and above. Moreover, XRD analysis was carried out using a Rigaku smart lab diffractometer (Rigaku, The Woodlands, TX, USA) to examine the metallurgical phases present on the coatings' surface in both as-deposited conditions and after exposure to 1000 hours of chloride corrosive conditions. The radiation was generated by Cu-Kα, and λ of K-α1 is 1.541Å, and λ of K-α2 is 1.544Å. The samples were scanned from the positions of (2θ) of 15° and stopped at the positions (2θ) of approximately 90° at room temperature with a step size of 0.0200°. The resulting XRD peaks were analyzed based on the inorganic crystal structure database (ICSD) and crystallography open database (COD). This step was crucial in determining and analyzing the behavior of the coatings under different exposure conditions.

Electrochemical Studies

The corrosion monitoring of the coatings was done by performing EIS. A set of 3 specimens from both Zn-15Al and Zn-Al pseudo alloy coatings were taken out of the spray chamber from salt spray and immersion exposure conditions at an interval of 200 hours to conduct EIS studies. A Gamry potentiostat (Reference 600) was employed to carry out the electrochemical testing. Using a $1cm^2$ working electrode area, the tests were conducted with a 5.0wt.% NaCl solution as the electrolyte (the same solution used for the salt spray chamber). A three-electrode cell setup was used, with the coating being investigated as the working electrode (WE), a platinum mesh utilized as the counter electrode (CE), and a saturated calomel electrode used as the reference electrode (RE). To eliminate the external interferences, the electrochemical cell was placed in a Faraday cage throughout the testing process. The EIS measurements were taken by applying a sinusoidal voltage signal (perturbation) with a 5-mV amplitude across a range of frequencies from 100kHz to 0.01Hz. PDS was performed (Ref 27) on the coatings before and after exposure to 1000 hours of salt spray and immersion exposures to record the changes in the corrosion potential, corrosion current, and rate of corrosion. PDS was run with a scan rate of 1mV/s from -0.4 to +0.8V with respect to open circuit potential (OCP).

Results and Discussion

SEM and EDS Analyses of the Undamaged Coatings

This section provides the results of the investigation into the effect of prolonged exposure to immersion and salt spray conditions obtained through SEM and EDS analyses. The assessment was carried out by analyzing the corrosion product formation, the relative oxidation levels, and the penetration of chloride ions for both Zn-15Al and Zn-Al pseudo alloy coatings in undamaged conditions. **Fig. 1 (a)** and **(b)** present the cross-sectional micrographs of the Zn-15Al coating after

being subjected to 1000 hours of immersion and salt spray (5wt.% NaCl) conditions, respectively. As seen in **Fig. 1 (a)** the corrosion product layer and the affected thickness of the coating appeared to be minimal, indicating better protection performance of the Zn-15Al coating when subjected to corrosion in immersion conditions. In immersion environments, the corrosion mechanism is typically driven by electrochemical reactions that occur at the metal-electrolyte interface (Ref 28). Zn-15Al coatings tend to have a higher corrosion potential which could have promoted the formation of a thin protective oxide layer on the surface of the coating, during initial exposure to immersion (Ref 13,29). In addition, the limited availability of oxygen in the immersion environment could have also contributed to the slower degradation of the Zn-15Al coating. Consequently, Zn-15Al coating exhibited improved performance, and therefore only a thin layer of coating appeared to be affected after 1000 hours of immersion exposure as depicted in the micrograph shown in **Fig. 1 (a)**.

In contrast, during salt spray exposure, the corrosion mechanism is primarily driven by the presence of chloride ions, and high chloride exposure, in addition to the continuously refreshed nature of the electrolyte interaction can accelerate the corrosion process and increase the aggressive nature of the environment (Ref 30). This could have led to the faster dissolution of the coating by adversely affecting a relatively higher thickness of the Zn-15Al coating as depicted in **Fig. *1* (b)** compared to immersion exposure. **Figures 1 (c) and (d)** display SEM images taken on the cross sections of the Zn-Al pseudo alloy coatings after 1000 hours of immersion and salt spray exposures, respectively. It can be seen in these images that the cross-section of the pseudo alloy coating of Zn and Al consists of islands of dark grey and light grey regions which correspond to the Al-rich and Zn-rich regions, respectively. The formation of a thin layer of corrosion products after exposure to both exposure conditions was visible at the considered magnification in Zn-Al

pseudo alloy coating which can be seen in Figs. 1 (c) and (d). Nevertheless, Fig. 1 (c) revealed the formation of a relatively thinner layer of corrosion products after 1000 hours of immersion exposure compared to the layer observed in Fig. 1 (d) following 1000 hours of salt spray exposure. As the governing factors differ for corrosion mechanisms in immersion and salt spray exposure conditions, the difference in the thickness of corrosion products formed during immersion and salt spray exposure conditions for Zn-Al pseudo alloy coatings can be attributed to the underlying corrosion mechanisms. Therefore, a thicker corrosion product layer after salt spray exposure can be due to the presence of chlorides and higher availability of oxygen which could have promoted the formation of more corrosion products of Zn and Al. However, due to the higher aluminum content in Zn-Al pseudo alloy coating, and the presence of Zn-rich and Al-rich clusters in the coating microstructure seen in **Figs. 1 (c) and (d)**, the formed corrosion products in both immersion and salt spray exposure conditions tend to have a more compact structure and lower porosity compared to Zn-15Al. Furthermore, the higher aluminum content in Zn-Al pseudo alloy coating could also facilitate the development of more protective oxide layers such as $Al(OH)_3$, on the coating surface during exposure to a corrosive medium demonstrated in some of the previous studies in the literature (Ref 15,16,19). The presence of this enhanced oxide layer can improve the barrier effect and thereby corrosion resistance of the coating in a salt spray environment for Zn-Al pseudo alloy coating.

Micrographs taken on the cross-section of Zn-15Al at a magnification of X100 after 1000 hours of exposure to salt spray indicated a reduction in coating thickness which can be seen in **Fig. 2 (d)** compared to its immersion counterpart which can be seen in **Fig. 2 (a)**, indicating active dissolution of the coating during salt spray exposure conditions. The aggressive nature of the salt spray on the Zn-15Al coatings can also be noticed from the EDS maps of oxygen and chloride

presented in **Fig. *2* (e) and (f)**. Please note that in **Figs. 2 and 3**, dashed lines have been incorporated into the EDS maps of elements to highlight the boundary between the coating and the epoxy. Upon comparing **Figs. 2 (b) and (e)**, it was evident that the Zn-15Al coating cross-section had undergone through-thickness oxidation both during salt spray and immersion exposures. However, little to no chloride penetration was observed for Zn-15Al during immersion exposure as presented in **Fig. 2 (c)**, and the presence of chloride ions in the cross-section of Zn-15Al coatings was observed after exposure to 1000 hours of salt spray which can be seen in **Fig. 2 (f)**. These observations provide additional evidence that the Zn-15Al coatings are more susceptible to chloride-induced damage during salt spray compared to immersion conditions even when subjected to the same concentration of electrolyte in both conditions.

To validate the compact and barrier-like characteristics of the corrosion products formed on the surface of the Zn-Al pseudo alloy coatings, EDS maps of oxygen and chloride were generated and are presented in **Fig. 3 (b~f)**. From **Fig. 3 (b) and (c)**, it was evident that Zn-Al pseudo alloy coatings showcased minimal oxidation and near absence of chlorides respectively following a rigorous 1000-hour immersion exposure. This signified the protective nature of the coating under immersion conditions. Furthermore, **Fig. 3 (e) and (f)** display an even more impressive resistance to oxidation and penetration of chlorides in the Zn-Al pseudo alloy coating after undergoing a 1000-hour salt spray exposure. These results highlight the coating's ability to withstand the corrosive effects of the salt spray environment, thus, solidifying its efficacy as a barrier against oxidation and chloride intrusion.

As assessed through SEM and EDS characterization, Zn-Al pseudo alloy coating demonstrated superior resistance during prolonged exposure to both immersion and salt spray conditions. In contrast, Zn-15Al coating exhibited superior performance during immersion

exposure when compared to salt spray exposure. The following section presents the analysis of the SEM and EDS results obtained from examining both coatings, specifically focusing on instances where there is damage present in the coatings, leading to the exposure of the substrate.

SEM and EDS Analyses of the Damaged Coatings

After the completion of the 1000-hour exposure period in immersion and salt spray conditions, digital images were captured to assess the condition of the damaged coatings. The set of images presented in **Fig. 4 (a~d) and 5 (a~d)** showcase the digital images of Zn-15Al coatings and Zn-Al pseudo alloy coatings, respectively. These images visually depict the coatings in their undamaged state, after the introduction of a defect through a scribe, and the visual transformations and formation of corrosion products on the exposed steel within the damaged coatings after enduring 1000 hours of immersion and salt spray exposures. **Figures 4 (c) and (d)** provide clear evidence that, in the salt spray exposure condition, the formation of higher white deposits was observed compared to the immersion exposure for the Zn-15Al coating, indicating the active dissolution of the coating in the salt spray exposure conditions. Likewise, a comparable behavior was observed for the Zn-Al pseudo alloy coatings. **Figures 5 (c) and (d)** provide a visual appearance of the damaged coating following 1000 hours of immersion exposure and salt spray exposure, respectively. On the surface of the damaged Zn-Al pseudo alloy coating, even after 1000 hours of salt spray exposure, the uncovered steel within the scribed portion remained visible. This observation indicated the formation of a lesser quantity of corrosion products compared to Zn-15Al coatings during salt spray exposure. This difference can be attributed to the higher aluminum content and the selective dissolution of zinc in the pseudo-alloy coating (Ref 16). Taking a broader perspective, it is crucial to emphasize that neither of the damaged coatings exhibited visible signs of rust on their surfaces under both exposure conditions. This noteworthy outcome

indicates the effective active cathodic protection provided by these coating systems in safeguarding the exposed substrate steel. To gain a more comprehensive understanding of the microstructural changes near the damaged areas in both coatings, a detailed analysis was conducted using SEM and EDS. These analyses aimed to delve into the behavior and protective performance of the damaged coatings during prolonged exposure to immersion and salt spray environments.

The cross-section micrographs of the damaged Zn-15Al coatings, following exposure to 1000 hours of immersion and salt spray are presented in **Fig. 6 (a~d)**. Specifically, **Fig. 6 (a)** showcases the coating exposed to immersion at low magnification of X30, providing an overall appearance of the damaged coating. As per **Fig. 6 (a)**, minimal to no corrosion or damage to the coating or steel near the exposed steel was evident during the 1000 hours of immersion. At X100 magnification, the micrograph depicted in **Fig. 6** (**b**) confirmed the formation of a thin layer of corrosion products on the coating's surface, while no accumulation of corrosion products was observed on the exposed steel. These observations signify the mild nature of the immersion exposure conditions for Zn-15Al coatings, emphasizing their efficient corrosion protection capability through cathodic protection mechanisms to shield the exposed steel from undergoing corrosion. On the other hand, the SEM micrograph in **Fig. 6 (c)** presents the overall view of the damaged Zn-15Al coating at X30 after 1000 hours of salt spray exposure. The micrograph clearly showed the presence of a thin layer of deposited corrosion products on the surface of the exposed steel. Additionally, the reduced thickness of the Zn-15Al coating surrounding the damaged area was distinctly visible in this image. Moreover, from the SEM image obtained at X100 magnification presented in **Fig. 6 (d)**, the coating appeared discolored and contained holes, serving as a clear indicator of degradation caused by the salt spray conditions. This visual evidence further

Formatted: Do not check spelling or grammar

underscores the aggressive nature of salt spray for Zn-15Al coatings, which promoted the active dissolution of the coating, thus providing sacrificial protection to the exposed steel. The EDS mapping of important elements including oxygen, chlorides, zinc, aluminum, and iron was carried out for the damaged Zn-15Al coatings following exposure to 1000-hour immersion and salt spray exposure conditions.

Figure 7 (b~f) presents the EDS maps of the damaged Zn-15Al coating following prolonged exposure to immersion conditions. Specifically, **Fig. 7 (b)** revealed that the Zn-15Al coating was heavily oxidized near the damaged portion. However, very little penetration of chlorides into the coating's cross-section was observed in **Fig. 7 (c)**. In addition, the combined EDS map of elements zinc and iron presented in **Fig. 7 (e)** confirmed the exposed steel in the damaged portion did not undergo any corrosion or form any rust. These findings serve as additional evidence of the effective cathodic protection offered by the Zn-15Al coating under immersion conditions. Overall, these EDS maps serve as additional confirmation as they demonstrate the absence of corrosion product accumulation on the exposed steel. This observation aligns with the earlier findings derived from the SEM images presented in **Fig. 6 (a) and (b),** reiterating the promising protection offered by Zn-15Al coatings to the exposed steel during accidental damage in an immersion environment. The EDS maps of the elements obtained from the damaged Zn-15Al after exposure to 1000 hours of salt spray are presented in **Fig. 8 (a~f)**. Contrary to the EDS maps of oxygen seen from immersion exposure presented in **Fig. 7 (b)**, in the case of salt spray exposed Zn-15Al coating, a very high concentration of oxygen was noticed across the coating cross-section near damage as presented in **Fig. 8 (b)**. In addition, the presence of chlorides throughout the entire coating thickness near the damage was also evident from EDS maps of the chloride ions presented in **Fig. 8 (c)**. Moreover, the accumulation of corrosion products on the exposed steel observed

Formatted: Font: Bold, Do not check spelling or grammar

Formatted: Font: Bold, Do not check spelling or grammar

Formatted: Do not check spelling or grammar

earlier in **Fig. 6 (c)** and **(d)** appeared to be the corrosion products of zinc, confirmed by the detection of zinc on the exposed steel as seen in the combined EDS map of zinc and iron presented in **Fig. 8 (e)**. In summary, the EDS analysis conducted on the damaged Zn-15Al coating after salt spray exposure suggests that the corrosion products were primarily composed of elements zinc, oxygen, and chlorine and confirmed the active anodic dissolution of the coating offering cathodic protection to exposed steel.

The findings obtained through SEM imaging of damaged Zn-Al pseudo alloy coatings following 1000 hours of immersion and salt spray exposures are presented in **Figs. 9 (a~d)**. Specifically, **Figs. 9 (a) and (b)** provide an overall view of the damaged Zn-Al pseudo alloy coating after immersion exposure, captured at magnifications of X50 and X100, respectively. Similar to the performance of the damaged Zn-15Al coating, the pseudo alloy coating also demonstrated remarkable resilience, exhibiting no signs of coating damage, rust formation, or deposition of corrosion products on the exposed substrate steel. Notably, **Fig. 9 (b)** revealed the presence of a thin layer of oxidation products on the surface of the Zn-Al pseudo alloy coating. Continuing the analysis, **Figs. 9 (c) and (d)** present SEM micrographs detailing the damaged Zn-Al pseudo alloy coating after 1000 hours of salt spray exposure, obtained at magnifications of X50 and X100, respectively. These micrographs provide clear visual evidence of a thicker layer of corrosion products on the coating's surface, as well as the formation of a protective barrier of corrosion products that shields the exposed steel. These observations underscore the remarkable corrosion protection capabilities of Zn-Al pseudo alloy coatings, which effectively employ cathodic protection mechanisms to shield the exposed steel from corrosion in both immersion and salt spray environments. Furthermore, to gain deeper insights into the distribution of various elements and the composition of the formed corrosion products, EDS analysis was conducted on

Formatted: Font: Bold, Do not check spelling or grammar

Formatted: Do not check spelling or grammar

the damaged coatings after immersion and salt spray exposures. This EDS analysis further allowed for a comprehensive understanding of the protection performance and visual representation of the elements present within the corrosion products formed on Zn-Al pseudo alloy coatings during exposure to a corrosive medium.

Figures 10 (b~e) and 11 (b~e) present the EDS maps of the damaged Zn-Al pseudo alloy coating after prolonged exposure to immersion and salt spray conditions, respectively. In particular, **Fig. 10 (b) and 11 (b)** illustrate that the pseudo-alloy coating experienced minimal oxidation in both environments, indicating the protective nature of the corrosion products formed on the surface of the coating, which effectively limits oxidation. Moreover, there was negligible penetration of chlorides into the cross-section of the coating observed in both exposure conditions, as depicted in **Fig. 10 (c) and 11 (c).** Furthermore, the EDS maps of zinc and aluminum in **Figs. 10 (d) and (e)** confirm the presence of zinc and aluminum clusters within the coating's cross-section respectively, which is the inherent property of the pseudo alloy coating (Ref 31). However, no zinc or aluminum was noticed on the exposed steel in the damaged area as per the elemental maps. This indicated that there was no accelerated dissolution of the coating during immersion exposure. Conversely, **Fig. 11 (d)** revealed the presence of zinc in the damaged portion of the coating, and **Fig. 11 (e)** suggested the detection of low-intensity aluminum in the exposed steel, implying the formation and deposition of corrosion products of both zinc and aluminum. The corrosion products act as a protective barrier on the exposed steel, preventing it from undergoing corrosion. These findings provide substantial evidence of the effective combined cathodic and barrier protection mechanisms offered by Zn-Al coatings to safeguard exposed steel in both immersion and salt spray exposure conditions and the observations align with the earlier findings derived from the SEM images presented, reinforcing the significant protection provided by Zn-Al

coatings to exposed steel in the event of accidental damage when serving under immersion and salt spray exposure conditions.

XRD Characterization of the Coatings

The X-ray diffraction (XRD) patterns of Zn-15Al and Zn-Al pseudo alloy coatings in their as-sprayed conditions are displayed in **Fig. 12**. The XRD patterns of both coatings exhibited identical peaks corresponding to the Al and Zn phases. These findings align with previous studies conducted on thermally sprayed Zn-Al coatings, which reported similar observations (Ref 32). Following exposure to 1000 hours of immersion conditions, the XRD spectra obtained from both coatings are presented in **Fig. 13**. For Zn-15Al coating, the diffraction pattern primarily consisted of Zn and Al peaks, along with a notable presence of weaker peaks corresponding to hydrozincite ($Zn_5(CO_3)_2(OH)_6$) and very faint peaks of simonkolleite ($Zn_5(OH)_8Cl_2{\cdot}H_2O$). On the other hand, the XRD pattern of the Zn-Al pseudo alloy coating after immersion exposure exhibited a good number of low-intensity peaks of simonkolleite and a few weaker peaks of hydrozincite, alongside the peaks of Zn and Al. Prior studies on Zn-Al coatings have identified hydrozincite and simonkolleite as the main compounds in corrosion products (Ref 16,19). The formation of hydrozincite and simonkolleite during the Zn or Zn-Al coatings corrosion in a chloride environment is influenced by various factors such as pH levels and wet/dry cycles (Ref 33,34). The absence of some of the distinct peaks corresponding to hydrozincite and simonkolleite in the corrosion products of these coatings may be attributed to factors such as their presence in an amorphous phase or as poorly defined crystals, leading to the absence or weak diffraction peaks (Ref 35). Nonetheless, it is essential to emphasize that both simonkolleite and hydrozincite are

stable corrosion products of zinc and can provide effective barrier protection. These results support the observations derived from the SEM and EDS analysis results presented in **Figs. 1 to 3**.

Furthermore, **Figs. 14 and 15** display the XRD spectra of the corrosion products formed on the surface of Zn-15Al and Zn-Al pseudo alloy coatings, respectively, after 1000 hours of salt spray exposure. The corrosion products in both coatings consisted of the same phases observed on the surfaces of the coatings after immersion exposure such as simonkolleite, and hydrozincite. Additional peaks corresponding to phases including zincite (ZnO), aluminum oxide (Al_2O_3), and sodium chloride (NaCl), along with a few peaks of Zn and Al were also observed on both the coatings after exposure to 1000 hours of salt spray indicating the active dissolution of the constituent metals. This led to the formation of different corrosion products on the surface of the coatings when exposed to the salt spray environment. Additionally, the XRD pattern from the corrosion products of the Zn-Al pseudo alloy coatings revealed peaks associated with aluminum hydroxide ($Al(OH)_3$). The presence of $Al(OH)_3$ had been shown to enhance the barrier performance of the coating as supported by previous studies (Ref 36,37). This was further evidenced by the SEM results and EDS maps presented in **Fig. 3**, which demonstrated minimal oxidation and absence of chloride penetration in Zn-Al pseudo alloy coatings after salt spray exposure.

EIS Studies on the Coatings

The corrosion resistance of Zn-15Al and Zn-Al pseudo alloy coatings was assessed through EIS studies during prolonged exposure to immersion and salt spray conditions. EIS characterization was conducted on both coatings in their initial as-sprayed state, as well as after subjecting them to varying durations of exposure (200, 400, 600, 800, and 1000 hours) in

immersion and salt spray environments. The obtained EIS data allowed for a comprehensive analysis of the corrosion behavior and the protective mechanisms provided by the coatings. The findings were presented in the form of Nyquist and Bode modulus plots, alongside an equivalent electrical circuit model (EEC), providing a thorough understanding of the coatings' performance.

The Nyquist plots and the Bode modulus plots obtained from Zn-15Al coatings during prolonged immersion exposure are presented in **Figs. 16 (a) and (b**) respectively. The Nyquist plots shown in **Fig. 16 (a)** consisted of two distinct semi-circle loops. The semi-circle corresponding to the higher studied frequency represents the properties of the coating and the semi-circle at the lower studied frequency provides information about the oxide or corrosion product layer and solution interface during the corrosion process (Ref 18). The overall dimension of the Nyquist plot obtained from the coating in the as-sprayed condition was much smaller, indicating that during early exposure periods, corrosion was initiated but without the formation of protective and stable corrosion products. The dimensions of the Nyquist plot increased consistently with an increase in the duration of immersion exposure until 1000 hours. This had been observed in several past EIS studies on Zn-15Al coatings, which demonstrate the occurrence of corrosion in the coating during initial exposure periods and subsequent deposition of the stable corrosion products covering the surface of the coating (Ref 38). As seen in the XRD analysis of the corrosion products formed on the surface of Zn-15Al coatings after 1000 hours of immersion exposure, the presence of hydrozincite and simonkolleite (see **Fig. 13**) contributed to blocking active sites for corrosion and increased corrosion resistance of the coating. This phenomenon was manifested as an increased diameter of the semi-circle loops, especially in the lower studied frequencies, which represented the protective nature of the formed oxide or corrosion product layer (Ref 39,40). However, the exact values of the impedance or corrosion resistance of the coating can’t be

quantified directly from the Nyquist plot. The Bode modulus plot in **Fig. 16 (b)** presents the changes in the impedance values over the studied frequencies after exposure to different durations of immersion exposure for the Zn-15Al coatings. The impedance value associated with corrosion products is observed at the lowest frequency studied (0.01Hz). These impedance values for Zn-15Al coatings after 1 hour of exposure (as-sprayed conditions) were found to be 405.0Ω-cm^2 which increased to 2228.2Ω-cm^2 after 1000 hours of immersion exposure in 5.0wt.% NaCl solution showing a 5-fold increase in the corrosion resistance during exposure to prolonged immersion conditions indicating the uniform deposition of the corrosion products covering the surface of the coating after prolonged exposure to immersion conditions (Ref 18).

The EIS plots of Zn-15Al coatings during prolonged exposure to salt spray conditions are shown in **Fig. 17**. Like the immersion conditions, the salt spray exposed coatings also exhibited an increase in the sizes of the semi-circle loops with an increase in exposure duration. However, the diameter of the semi-circle loops was much smaller compared to those seen during the immersion exposure (see **Fig. 17 (a)**). The exact value of the impedance at 0.01Hz for Zn-15Al coatings after 1000 hours of salt spray exposure was found to be 854.6Ω-cm^2, approximately 3 times less than what had been observed for the immersion exposure conditions. This observation suggested the vulnerability of the Zn-15Al coatings to salt spray environments, where the thin electrolyte that is constantly refreshed might have prevented or washed off the partially formed corrosion product layer and allowed chlorides to penetrate through the porous coating structure which reduced the overall barrier protection/ impedance of the coating compared to immersion exposure conditions. The EIS data depicting the behavior of Zn-15Al coatings in immersion and salt spray exposure is corroborated by the SEM and EDS analysis presented in **Figs. 1 and 2**. These observations show the penetration of chloride ions and increased oxidation in the cross-section of

the Zn-15Al coating after 1000 hours of salt spray, compared to 1000 hours of immersion exposure.

Figure 18 presents the EIS graphs for Zn-Al pseudo alloy coatings during 1000 hours of immersion exposure in 5wt.% NaCl solution. The Nyquist plots of the coating displayed two different semi-circle loops at each exposure period and the size of the semi-circle loop at lower studied frequencies increased with an increase in the duration of exposure to the immersion environment from 1 hour to 1000 hours which can be seen in **Fig. 18 (a)**. As mentioned previously, the semi-circle corresponds to the lower studied frequencies representing the nature of the corrosion product layer/ oxidation layer. The increase in the size of this loop with an increase in the duration of exposure suggests the protective or barrier nature of the formed products. As seen earlier, the XRD pattern from Zn-Al pseudo alloy coating after 1000 hours of immersion exposure was similar to Zn-15Al after 1000 hours of immersion exposure and exhibited peaks of protective corrosion products including simonkolleite and hydrozincite. The increased capacitance loop or barrier action with an increase in immersion exposure observed in Nyquist plots can be attributed to the presence of these stable corrosion products on the coating's surface. For Zn-Al pseudo alloy coating, the impedance values correspond to 0.01Hz after 1 hour and 1000 hours of immersion exposure obtained from the Bode modulus plot presented in **Fig. 18 (b)** were 406.0Ω-cm^2 and 1151.5Ω-cm^2 respectively. These values indicated a 3 times better barrier performance of the formed corrosion products after 1000 hours of immersion exposure than its as-sprayed conditions.

The Nyquist plots of the Zn-Al pseudo alloy coatings obtained from EIS data during 1000 hours of salt spray exposure are presented in **Fig. 19 (a)**. This Nyquist plot exhibited a trend similar to what was observed for Zn-15Al coatings in both immersion and salt spray exposure and Zn-Al pseudo alloy coatings during immersion exposure. An increase in the size of the capacitive loop at

the lower studied frequency with an increase in the exposure durations up to 1000 hours. However, the size of the semi-circle loop was much higher than what had been noticed earlier, suggesting the formation of a more adherent and compact layer of corrosion products on the surface of Zn-Al pseudo alloy coatings compared to Zn-15Al coatings during extended exposure to salt spray conditions. As discussed previously, the primary corrosion mechanism during salt spray exposure is driven by the presence of chloride ions and the interaction of a continuously refreshing thin electrolyte layer. Zn-Al pseudo alloy coatings with a higher aluminum content compared to Zn-15Al coatings tend to have a more compact microstructure and a lower porosity, which can help limit the penetration of chloride ions into the coating (Ref 16). In addition, the higher aluminum content can promote the formation of more protective oxides of aluminum on the coating's surface, which further improves the coating's performance during prolonged exposure to salt spray exposure conditions (Ref 38). This premise was confirmed by the XRD spectrum of corrosion products formed on Zn-Al pseudo alloy coating after 1000 hours of salt spray exposure, which consisted of peaks corresponding to Al $(OH)_3$ in addition to other stable products including hydrozincite and simonkolleite which were observed for all other conditions. The SEM images from the coating after 1000 hours of exposure also indicated the presence of a thin layer of protective oxides on the coating's surface and the corresponding EDS maps showed very little oxidation and no penetration of chloride ions into the coating's cross-section substantiating the protective barrier nature of the formed products during salt spray exposure. Therefore, the impedance value of the Zn-Al pseudo alloy coatings at 0.01Hz observed from Bode modulus plot in **Fig. 19 (b)** was found to be 2.5 times higher compared to Zn-15Al coatings after 1000 hours of salt spray exposure.

Under controlled conditions, where factors such as temperature, humidity, pH, and electrolyte concentration remained constant, the EIS study of Zn-15Al and Zn-Al pseudo alloy coatings during prolonged exposure to salt spray and immersion environments unveiled notable differences in performance. Zn-15Al coatings exhibited better performance during immersion while showing relatively poor performance in salt spray conditions. Conversely, Zn-Al pseudo alloy coatings showcased promising performance during immersion and demonstrated significantly improved protection against salt spray exposures. These findings highlight the influence of exposure conditions on the performance evaluation of the coatings and the potential benefits of using an appropriate coating system for a particular environment. The difference in the coatings' composition, microstructure, and the difference in electrolyte layer interaction governed the protection performance of the coatings in this study. Therefore, evaluating zinc coatings with lower aluminum content such as Zn-15Al in salt spray conditions results in relatively poor performance, and testing the same coating in an immersion environment suggests a much better long-term protection from the coating. Conversely, the Zn-Al pseudo alloy coating, although performed well in both exposure conditions, shows a much better protection performance during salt spray compared to immersion exposures. Notably, it is worth mentioning that both coatings displayed qualitatively similar Nyquist plots under all exposure conditions indicating that both systems utilize identical corrosion mechanisms. However, the key distinction lies in the size of the semi-circles observed in the Nyquist plots and the magnitude of impedance values obtained from the Bode plots. This common corrosion mechanism observed in the coatings was characterized using an EEC model, derived from the EIS data. The EEC model, illustrating the corrosion behavior of the two coating systems in both immersion and salt spray exposures, is presented in **Fig. 20**. The EEC model best fits the EIS data in **Fig. 20** where two EECs are connected to each

other. The R_c of the first circuit is connected in series with the R_{ct} of the second circuit. The first circuit presents the characteristics of the coating attributed to the coating's polarization resistance and the second circuit is due to the deposition of corrosion products caused by R_{ct}. Descriptions of different electrical elements used in the EEC are as follows: The R_s corresponds to the solution resistance, and R_c and CPE_{po} correspond to the resistance and the constant phase element of the coating. R_{ct} and CPE_{dl} are the charge transfer resistance and double-layer capacitance of the corrosion products deposited on the coating (Ref 41,42). In EEC, CPE is a generalized form of a non-ideal capacitor/ effective capacitance, that can account for a wide range of impedance responses and is calculated by the imaginary impedance using the following equation when $n \neq 1$ (Ref 43,44) :

$$CPE_{eff} = \sin\left(\frac{n\pi}{2}\right)\frac{-1}{Z_j(f)(2\pi f)^n} \quad \text{(Eq 1)}$$

where, Z_j is the imaginary impedance, n is the CPE exponent, and f is the frequency. The values of the electrochemical parameters that best fit the EEC model for both coatings in the two exposure conditions are presented in **Table 2**. As seen in **Table 2**, the values of R_s remained relatively consistent with minimal variation across the different exposure periods for both Zn-15Al and Zn-Al pseudo alloy coatings. However, when analyzing R_{ct}, it was evident that although all coatings showed an overall increase in R_{ct}, the magnitude of the increase varied significantly depending on the specific exposure condition and coating type. For example, during immersion exposure, Zn-15Al exhibited an increase in R_{ct} from 806.90Ω-cm^2 to 3804.00Ω-cm^2, while during salt spray exposure, there was a gradual increase up to only 1580Ω-cm^2 at the end of 1000 hours. On the

other hand, for Zn-Al pseudo alloy coatings, R_{ct} increased significantly with an increase in exposure period from 952Ω-cm^2 to 4150Ω-cm^2 during salt spray exposure and it increased from 494.30Ω-cm^2 to 1784.00Ω-cm^2 during immersion exposure. Additionally, the values of CPE_{po} and CPE_{dl} demonstrated a decreasing trend as the exposure periods increased. This suggested that the corrosion products became more homogenous, and adherent, and acted as a barrier with an increase in exposure periods up to 1000 hours, impeding the movement of ions and electrons. As a result, the charge transfer resistance (R_{ct}) increased, indicating a reduction in the ability of the coatings to transfer charges. Furthermore, the decreasing values of CPE indicate a decrease in the capacitance behavior within the coatings. In summary, the EIS analysis indicated that while both coatings offer identical protection mechanisms during prolonged exposure conditions, their effectiveness in corrosion protection significantly depends on the type of exposure and this perfectly aligned with all the characterization results discussed in the earlier sections.

Polarization Behavior

Figures 21 and 22 present the potentiodynamic polarization curves of the Zn-15Al and Zn-Al pseudo alloy coatings respectively. In **Fig. 21**, the polarization curves of the Zn-15Al coatings are shown for unexposed conditions, as well as after 1000 hours of immersion and salt spray exposure. Notably, the Zn-15Al coating demonstrated a passivation tendency during the as-deposited state, which was exposed to the electrolyte for only 1 hour to stabilize the open circuit potential (OCP). This passivation behavior can be attributed to the formation of oxidation products of zinc, resulting in a small passivation region on the anodic polarization curve. For this condition, the corrosion potential (E_{corr}) was recorded as -1.26V, while the corrosion current (i_{corr}) was measured as 4.53µA/cm^2. The values of the E_{corr} and i_{corr} obtained from Tafel extrapolation at different exposure conditions are presented in **Table 3**. Upon exposure to the corrosive

environments, the E_{corr} value shifted to a more positive direction for Zn-15Al coating, indicating the formation of a barrier film, and or corrosion products precipitation on the surface of the coating. Specifically, after immersion exposure, the E_{corr} value changed to -1.24V, while after salt spray exposure, it shifted to -1.07V. However, the i_{corr} value of the Zn-15Al coating showed a slight increase after 1000 hours of immersion exposure (18.49µA/cm^2) and a substantial increase after 1000 hours of salt spray exposure (111.00µA/cm^2). This implied that the formed corrosion products on the surface of the Zn-15Al coating were either more porous or distributed unevenly over the coating's surface, especially when exposed to the salt spray environment. The increase in i_{corr} can also be attributed to the positive shift in the E_{corr} which creates a higher driving force for the migration of chloride ions towards the metal surface, thereby promoting accelerated corrosion rates (Ref 45,46). Particularly, for samples exposed to 1000 hours of salt spray conditions, the higher positive shift in the potential led to increased migration of ions and consequently higher corrosion current values signifying a faster deterioration for the Zn-15Al coatings in salt spray. The results from the polarization scanning of the Zn-15Al coating align with the findings from the EIS analysis of the same coating. Both tests indicated a much better corrosion protection performance of the coating following 1000 hours of immersion conditions compared to 1000 hours of salt spray exposure conditions.

Figure 22 displays the polarization curves for the Zn-Al pseudo alloy coatings before and after 1000 hours of immersion and salt spray exposures. As seen in **Table 3**, the E_{corr} value for the coating remained consistent at -1.25V before and after immersion exposure. However, following 1000 hours of salt spray exposure, there was a noticeable shift towards a more positive direction, reaching -1.11V, similar to the E_{corr} trend observed for the Zn-15Al coatings. While the coating exhibited an increase in i_{corr} values after exposure to 1000 hours of corrosion, the i_{corr} value after

1000 hours of immersion was found to be comparable to that of the Zn-15Al coating. In contrast, under salt spray exposure conditions, the i_{corr} value for the Zn-Al pseudo alloy coatings was significantly lower, approximately 15 times less than those of the Zn-15Al coating. This substantial difference suggested the development of a more protective barrier layer of corrosion products on the surface of the Zn-Al pseudo alloy coatings following salt spray exposure. The findings from XRD analysis of the Zn-Al pseudo alloy coating, which confirmed the presence of Al $(OH)_3$, aligned with this observation. Additionally, the SEM and EDS analysis results further strengthen the evidence for the protective nature of the formed corrosion product layer which showed no signs of chloride ion penetration into the coating cross-section and minimal oxidation after 1000 hours of salt spray exposure. The polarization behavior of the coatings is consistent with the findings obtained from other characterization tests, indicating that both Zn-15Al and Zn-Al pseudo alloy coatings provide promising corrosion protection during immersion exposure and yield comparable results. However, when it comes to salt spray testing conditions, the Zn-Al pseudo alloy coatings demonstrate superior corrosion protection compared to the Zn-15Al coatings. This emphasizes the significance of considering exposure conditions when evaluating the long-term performance of the thermally sprayed Zn-Al coatings with varying compositions of Zn and Al.

Conclusions

This comprehensive study investigated the influence of corrosion testing conditions on the long-term performance evaluation of wire-arc sprayed Zn-Al coatings, specifically Zn-15Al and Zn-Al pseudo alloy coatings with similar thickness but varying proportions of Zn and Al and different microstructural arrangements. The study specifically compared the observations from prolonged salt spray and immersion testing conducted under identical conditions. The significant findings and conclusions derived from this research are:

1. The protection performance of the sacrificial coatings of Zn-Al was shown to be influenced by the exposure conditions. The Zn-15Al coatings, with higher zinc content, exhibited superior behavior during immersion testing compared to salt spray. Whereas the Zn-Al pseudo alloy coatings, with higher aluminum content (approximately 37%) demonstrated better corrosion protection specifically during salt spray testing.
2. The self-sealing of the coatings due to the precipitation of stable corrosion products such as simonkolleite and hydrozincite was favored during the immersion test in a bulk stagnant electrolyte which provided a substantial contribution to the improved corrosion resistance for both coatings, particularly for Zn-15Al.
3. During salt spray testing, the continuously refreshed electrolyte prevented the uniform accumulation of stable corrosion products, allowing chlorides to penetrate the coating cross-section and accelerating the corrosion rate. As a result, the Zn-15Al coating experienced faster dissolution under salt spray conditions. On the other hand, the salt spray facilitated the formation of $Al(OH)_3$ along with other stable corrosion products for Zn-Al pseudo alloy coatings, resulting in enhanced corrosion resistance and improved protection properties.
4. The behavior of the damaged coatings remained consistent with that of their un-damaged counterparts during prolonged exposure to both immersion and salt spray conditions.
5. The exposure conditions had minimal impact on the qualitative EIS response of both coatings, demonstrating similar protection mechanisms and equivalent circuit models for salt spray and immersion environments. This suggested the formation of protective corrosion products during prolonged exposure in both coating systems. However, a notable difference in protection performance was observed when quantitatively assessing the

coatings using electrochemical parameters obtained from EIS, PDS, and other characterization tests.

The detailed findings emphasize the critical role of exposure conditions in predicting the long-term performance of Zn-15Al and Zn-Al pseudo alloy coatings and their effectiveness in safeguarding against oxidation and chloride penetration, bolstering their reputation as a reliable and corrosion-resistant solution. The thorough characterization and analysis performed in this study provide valuable insights into the coatings' behavior and performance, unveiling their unique strengths and distinct capabilities under different exposure conditions.

CRediT authorship contribution statement

Ratna Yasoda: Data curation, Methodology, Formal analysis, Investigation, Writing - original draft, Writing - review & editing. **Ying Huang:** Project administration, Funding acquisition, Supervision, Writing - review & editing. **Xiaoning Qi:** Supervision, Writing -review & editing.

Declaration of interest

The authors declare that they have no known competing financial interests or personal relationships that could have appeared to influence the work reported in this paper.

Acknowledgments

This work was supported by the National Science Foundation under Grant No. CMMI-1750316 and OIA-2119691. The findings and opinions expressed in this article are those of the authors only and do not necessarily reflect the views of the sponsors.

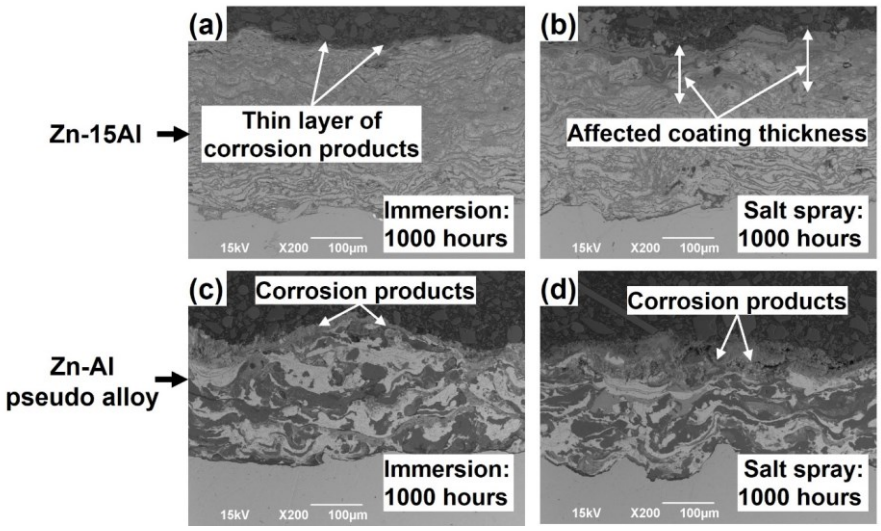

Fig. 1. Zn-15Al coating cross-section: (a) After 1000 hours of immersion exposure and (b) After 1000 hours of salt spray exposure. **Zn-Al pseudo alloy coating cross-section**: (c) After 1000 hours of immersion exposure and (d) After 1000 hours of salt spray exposure.

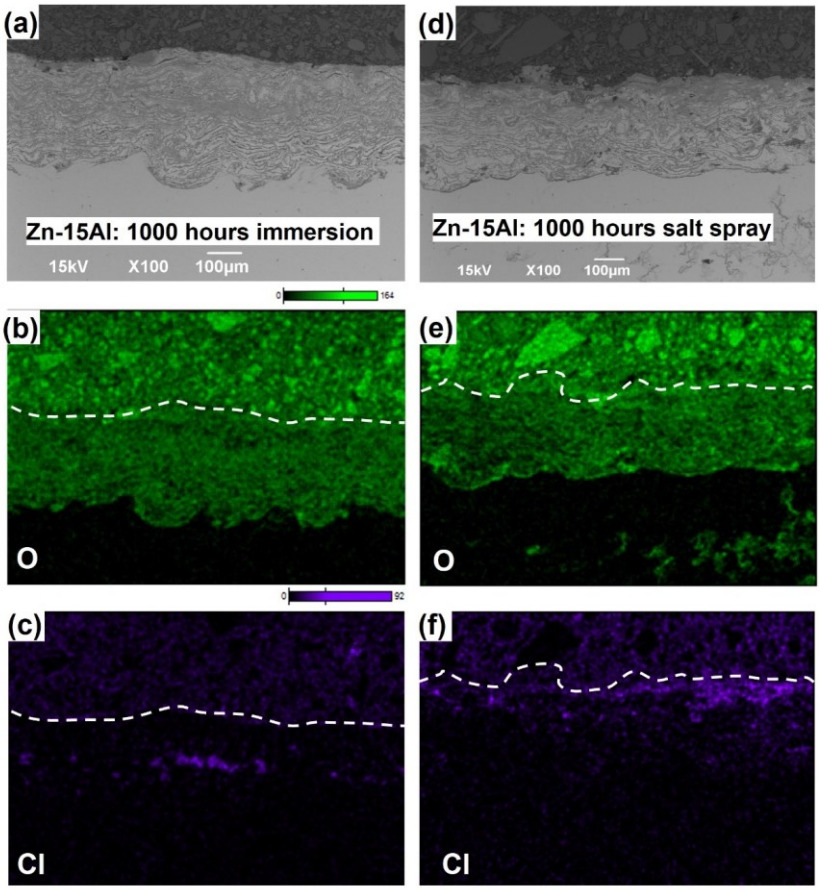

Fig. 2. Zn-15Al coating: (a) Cross-sectional micrograph after 1000 hours of immersion (b) EDS map of oxygen after 1000 hours of immersion (c) EDS map of chlorides after 1000 hours of immersion, (d) Cross-sectional micrograph after 1000 hours of salt spray (e) EDS map of oxygen corresponding to 1000 hours of salt spray (f) EDS map of chlorides corresponding to 1000 hours of salt spray.

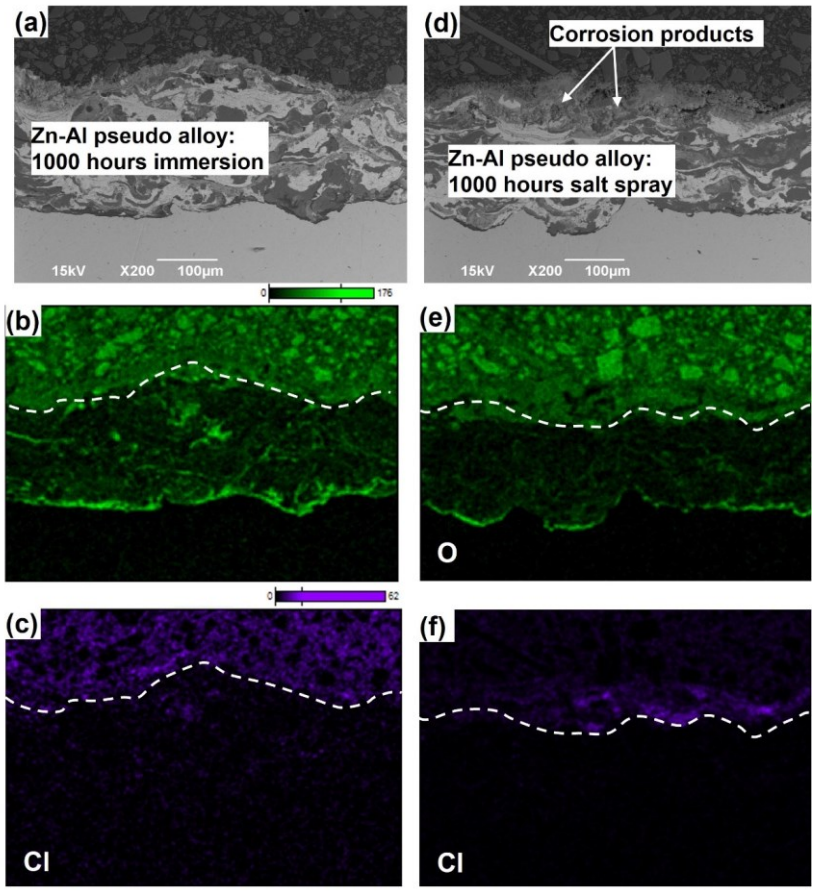

Fig. 3. Zn-Al pseudo alloy coating: (a) Cross-sectional micrograph after 1000 hours of immersion (b) EDS map of oxygen after 1000 hours of immersion (c) EDS map of chlorides after 1000 hours of immersion, (d) Cross-sectional micrograph after 1000 hours of salt spray (e) EDS map of oxygen corresponding to 1000 hours of salt spray (f) EDS map of chlorides corresponding to 1000 hours of salt spray.

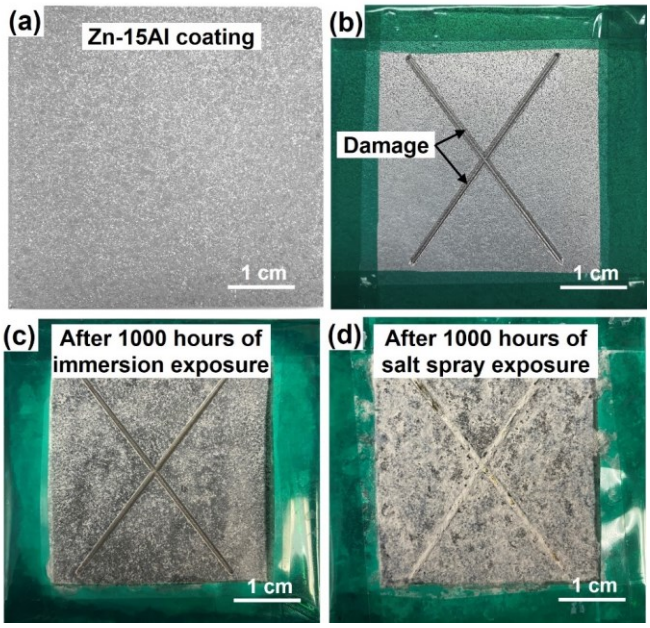

Fig. 4. Digital images of Zn-15Al coating under various conditions: (a) Initial as-sprayed condition (b) As-sprayed condition with intentionally machined damage, (c) Condition of the coating and associated damage after 1000 hours of immersion exposure, (d) Condition of the coating and damage with accumulated corrosion products after1000 hours of salt spray exposure.

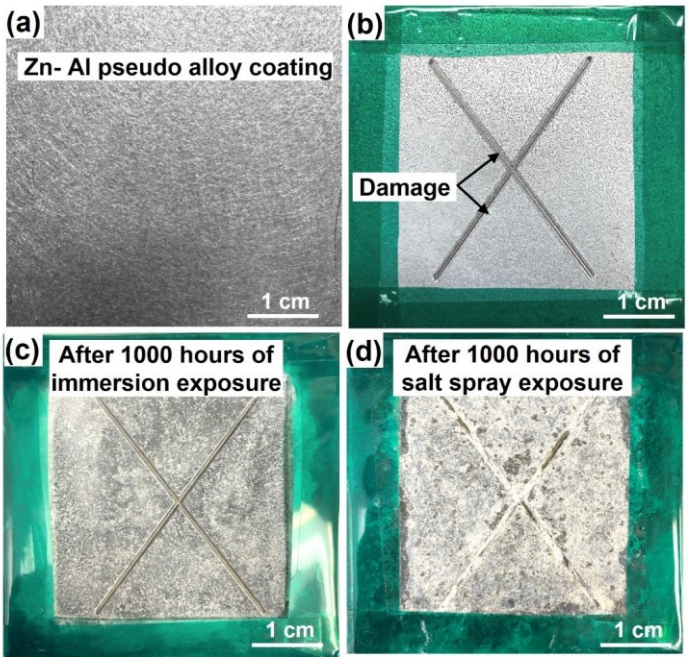

Fig. 5. Digital images of Zn-Al pseudo alloy coating under various conditions: (a) Initial as-sprayed condition (b) As-sprayed condition with intentionally machined damage, (c) Condition of the coating and associated damage after 1000 hours of immersion exposure, (d) Condition of the coating and damage with accumulated corrosion products after1000 hours of salt spray exposure.

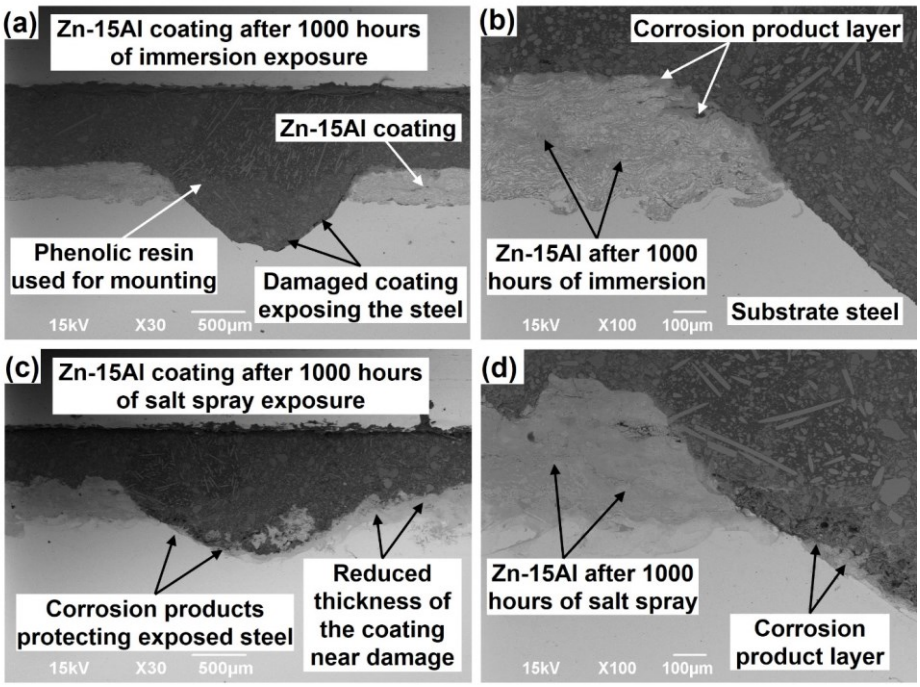

Fig. 6. Zn-15Al coating: (a) Low-magnification cross-sectional micrograph displaying the overall condition of the damaged coating after 1000 hours of immersion exposure, (b) Cross-sectional micrograph at 100X magnification providing a detailed view of the coating, substrate, and damaged area of the coating after 1000 hours of immersion exposure, (c) Low-magnification cross-sectional micrograph presenting a comprehensive view of the damaged coating after 1000 hours of salt spray exposure, (d) Cross-sectional micrograph at 100X magnification showcasing the coating, substrate, and damaged area of the coating after 1000 hours of salt spray exposure.

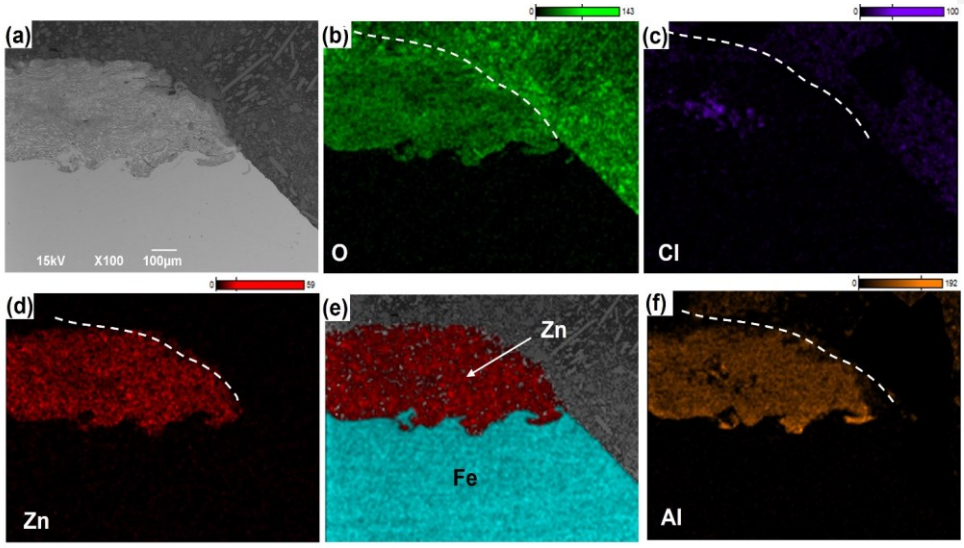

Fig. 7. Zn-15Al coating with damage after exposure to 1000 hours of immersion testing: (a) Cross-sectional micrograph of the coating utilized for EDS elemental mapping, and corresponding (b) EDS map of oxygen, (c) EDS map of chlorides, (d) EDS map of zinc, (e) combined EDS map of elements iron and zinc, and (f) EDS map of aluminum.

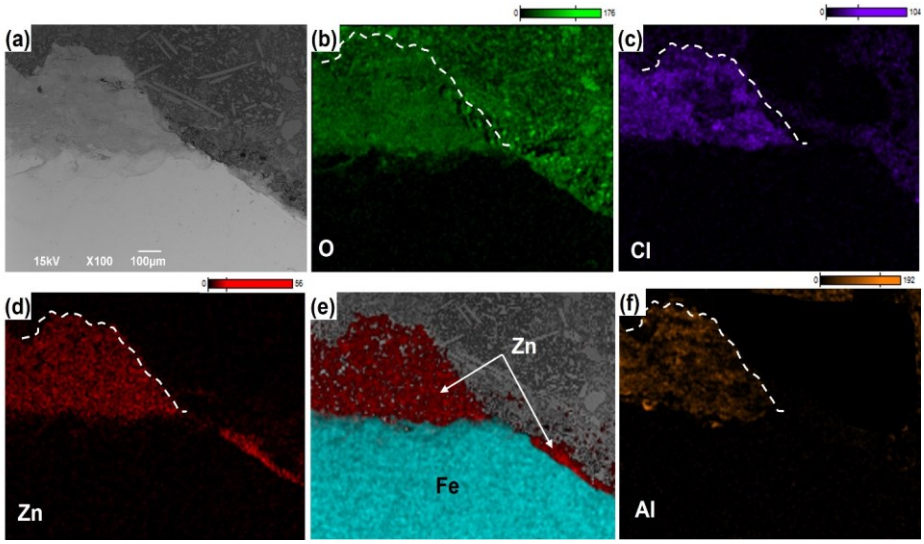

Fig. 8. Zn-15Al coating with damage after exposure to 1000 hours of salt spray testing: (a) Cross-sectional micrograph of the coating utilized for EDS elemental mapping, and corresponding (b) EDS map of oxygen, (c) EDS map of chlorides, (d) EDS map of zinc, (e) combined EDS map of elements iron and zinc, and (f) EDS map of aluminum.

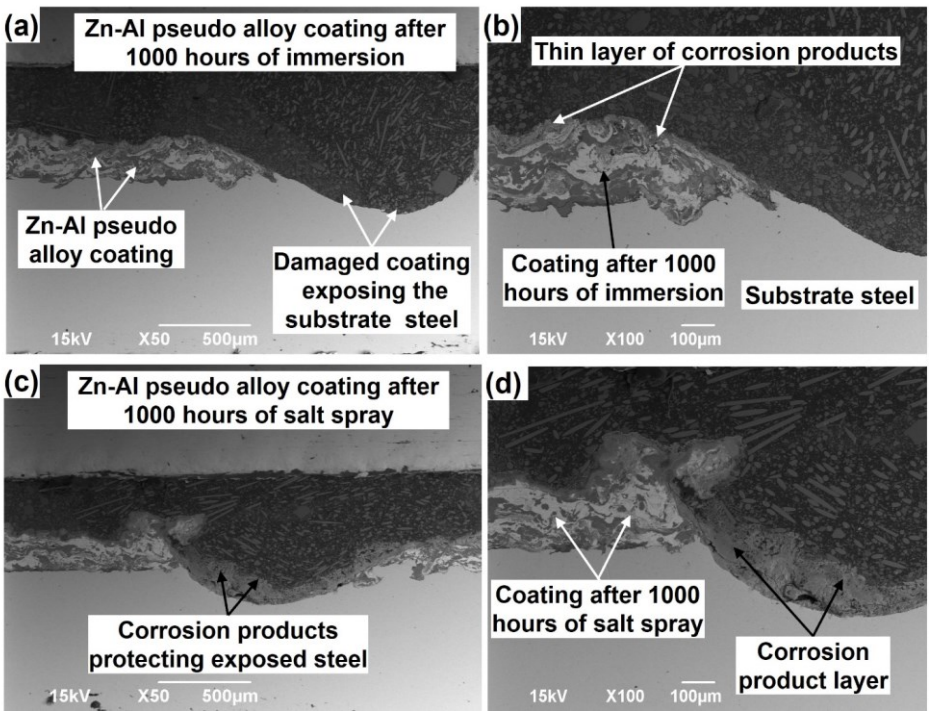

Fig. 9. Zn-Al pseudo alloy coating: (a) Low-magnification cross-sectional micrograph displaying the overall condition of the damaged coating after 1000 hours of immersion exposure, (b) Cross-sectional micrograph at 100X magnification providing a detailed view of the coating, substrate, and damaged area of the coating after 1000 hours of immersion exposure, (c) Low-magnification cross-sectional micrograph presenting a comprehensive view of the damaged coating after 1000 hours of salt spray exposure, (d) Cross-sectional micrograph at 100X magnification showcasing the coating, substrate, and damaged area of the coating after 1000 hours of salt spray exposure.

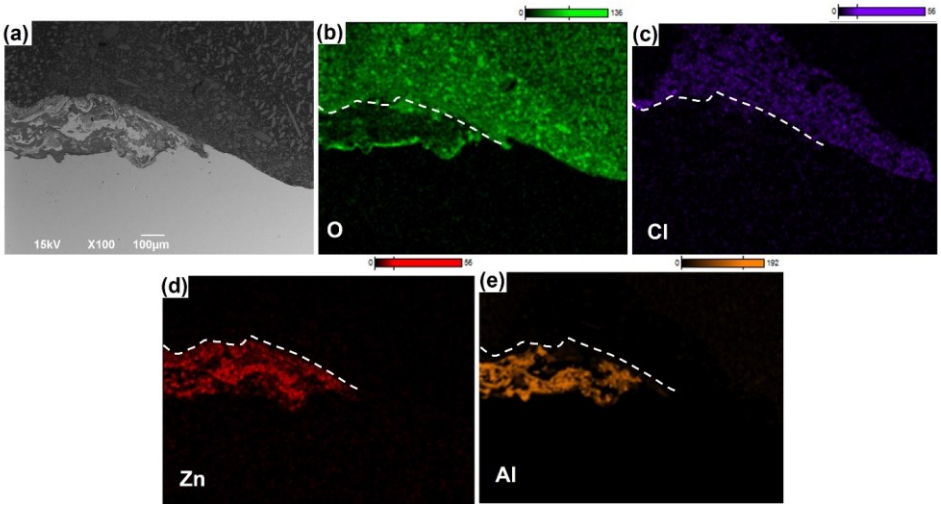

Fig. 10. Zn-Al pseudo alloy coating with damage after exposure to 1000 hours of immersion testing: (a) Cross-sectional micrograph of the coating utilized for EDS elemental mapping, and corresponding (b) EDS map of oxygen, (c) EDS map of chlorides, (d) EDS map of zinc, and (e) EDS map of aluminum.

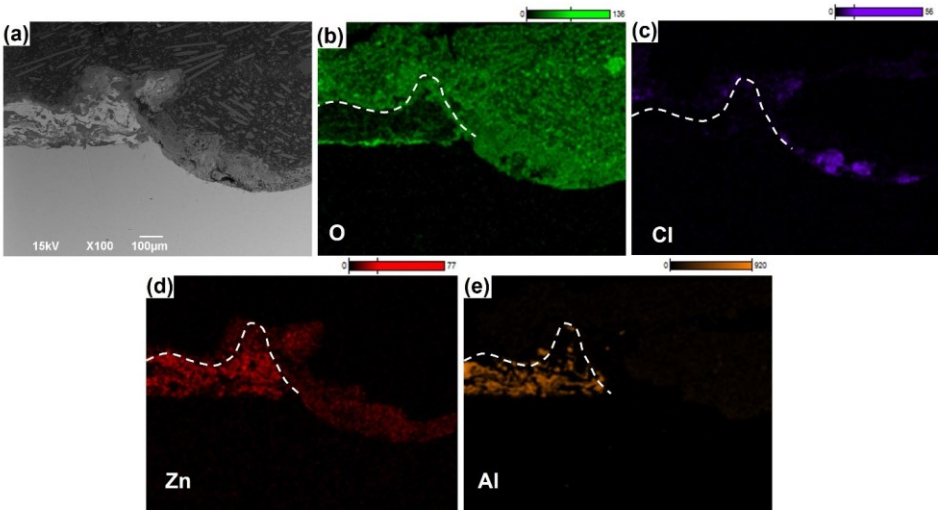

Fig. 11. Zn-Al pseudo alloy coating with damage after exposure to 1000 hours of salt spray testing: (a) Cross-sectional micrograph of the coating utilized for EDS elemental mapping, and corresponding (b) EDS map of oxygen, (c) EDS map of chlorides, (d) EDS map of zinc, and (e) EDS map of aluminum.

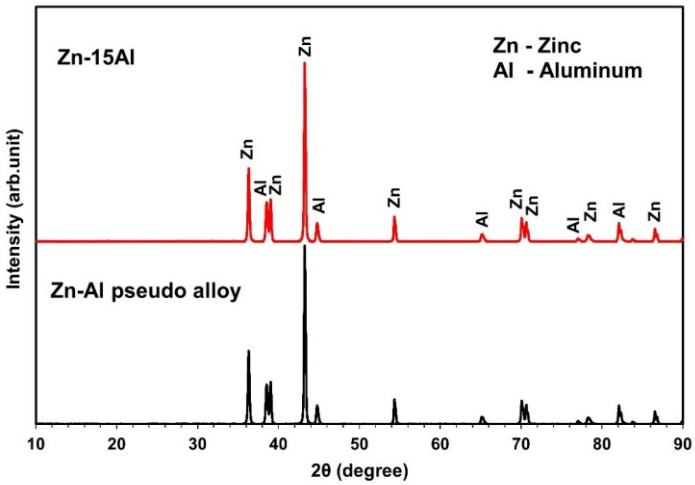

Fig. 12. XRD spectrum showing the phases present in the Zn-15Al and Zn-Al pseudo alloy coatings in their as-sprayed state.

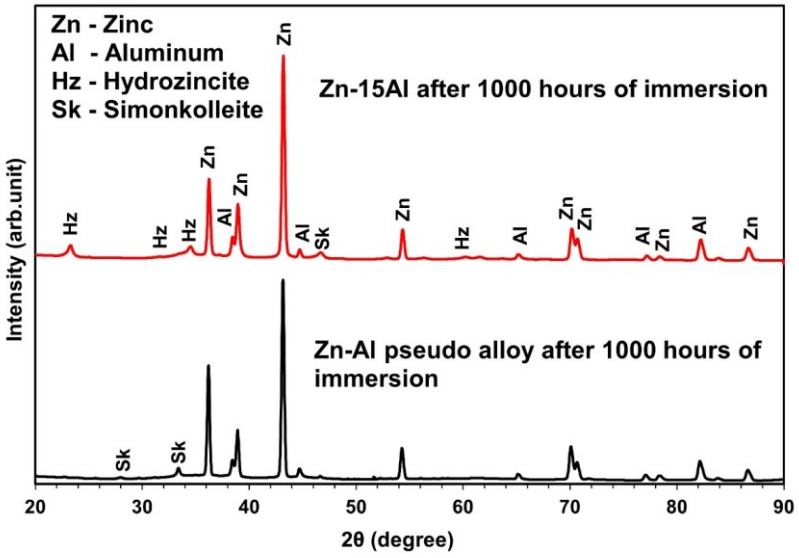

Fig. 13. XRD spectrum of Zn-15Al and Zn-Al pseudo alloy coatings following exposure to 1000 hours of immersion conditions.

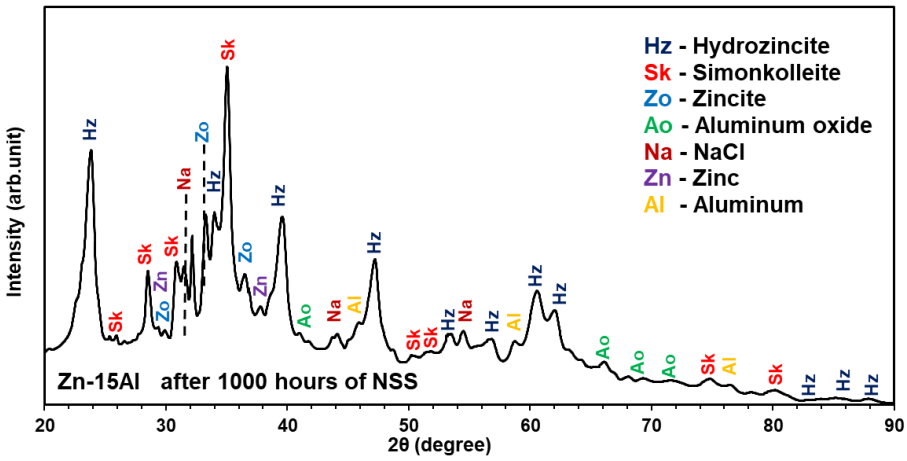

Fig. 14. XRD spectrum of Zn-15Al coating following exposure to 1000 hours of salt spray conditions.

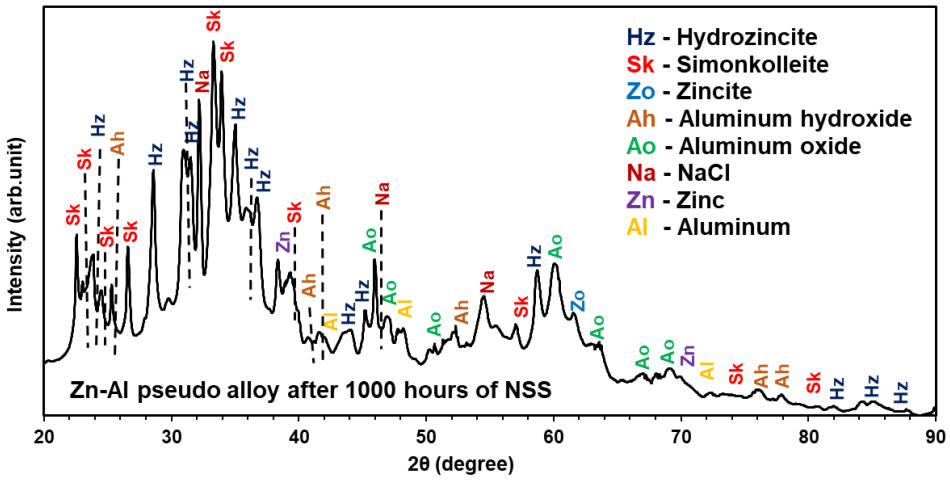

Fig. 15. XRD spectrum of Zn-Al pseudo alloy coating following exposure to 1000 hours of salt spray conditions.

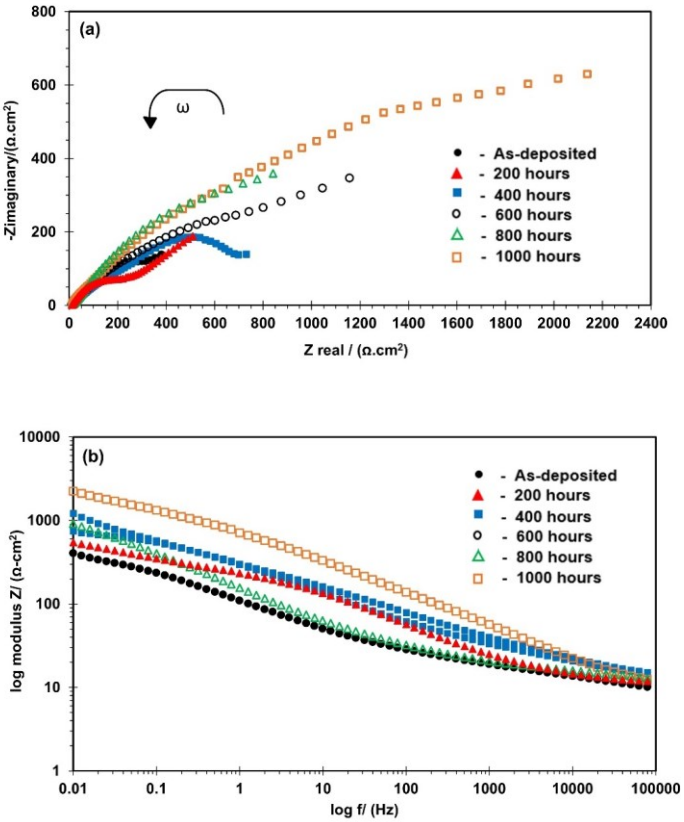

Fig. 16. Zn-15Al coatings: (a) Nyquist plots and (b) Bode modulus plots after being subjected to different periods of immersion exposure.

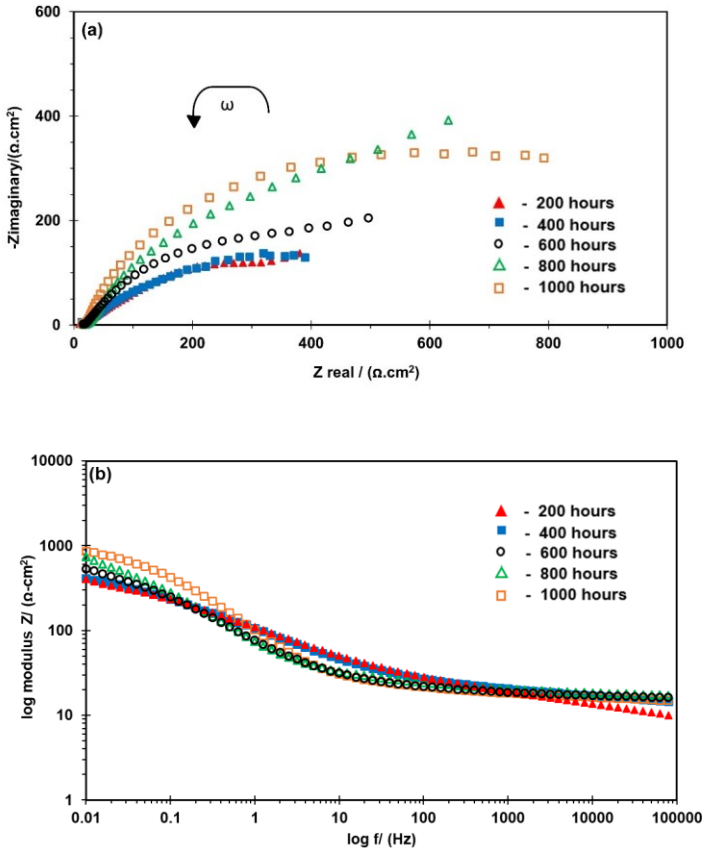

Fig. 17. Zn-15Al coatings: (a) Nyquist plots and (b) Bode modulus plots after being subjected to different periods of salt spray exposure.

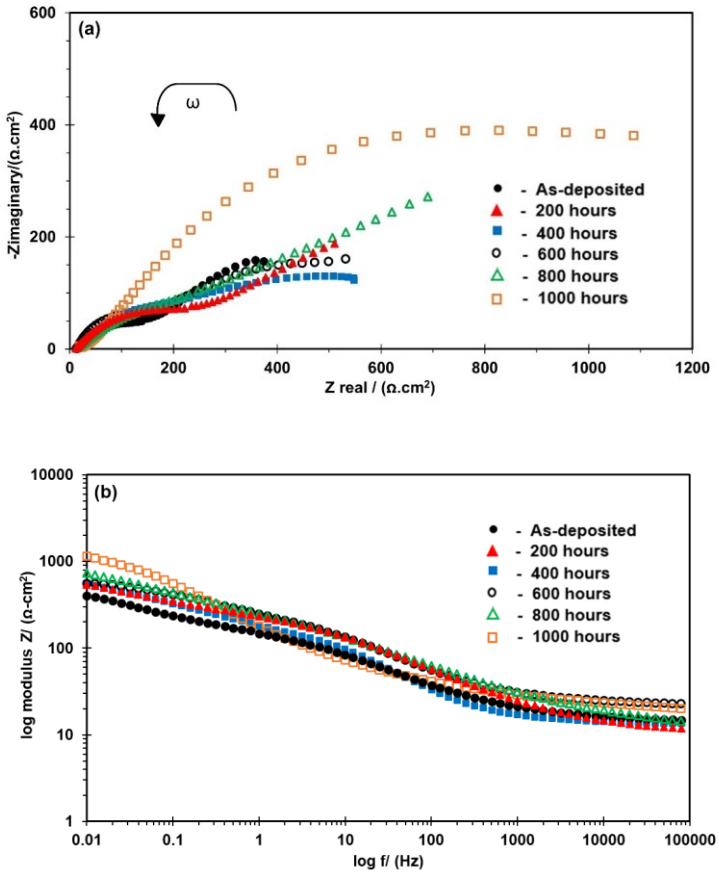

Fig. 18. Zn-Al pseudo alloy coatings: (a) Nyquist plots and (b) Bode modulus plots after being subjected to different periods of immersion exposure.

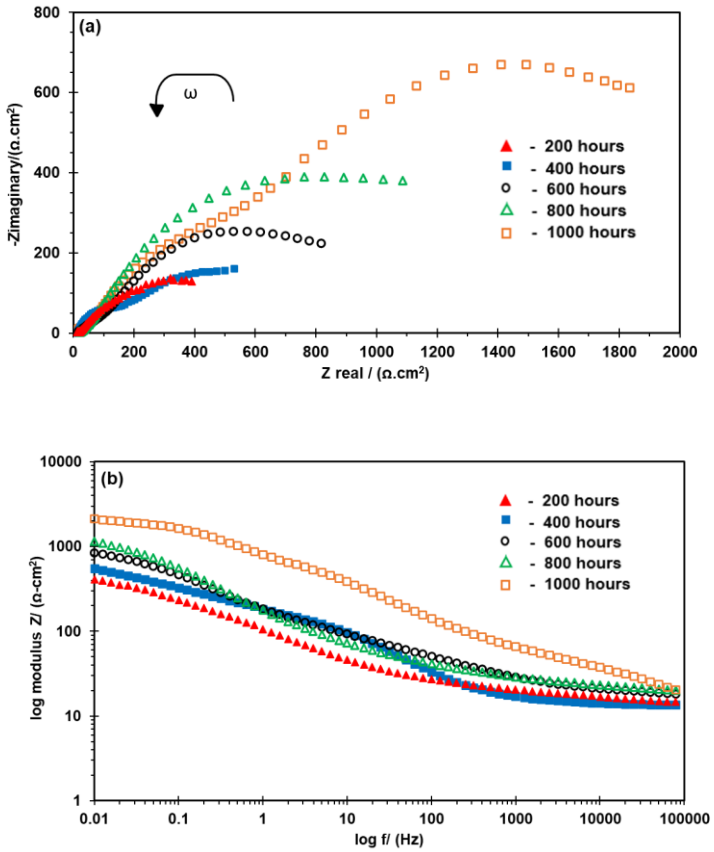

Fig. 19. Zn-Al pseudo alloy coatings: (a) Nyquist plots and (b) Bode modulus plots after being subjected to different periods of salt spray exposure.

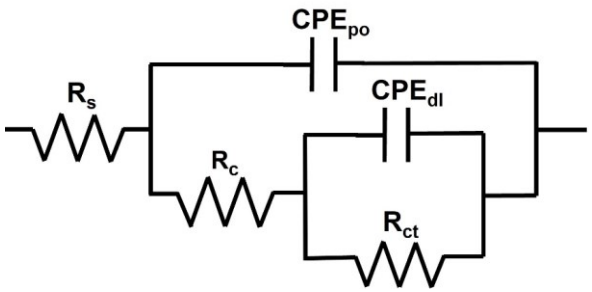

Fig. 20. EEC of the Zn-15Al and Zn-Al pseudo alloy coatings with different exposure periods to immersion and salt spray exposure conditions.

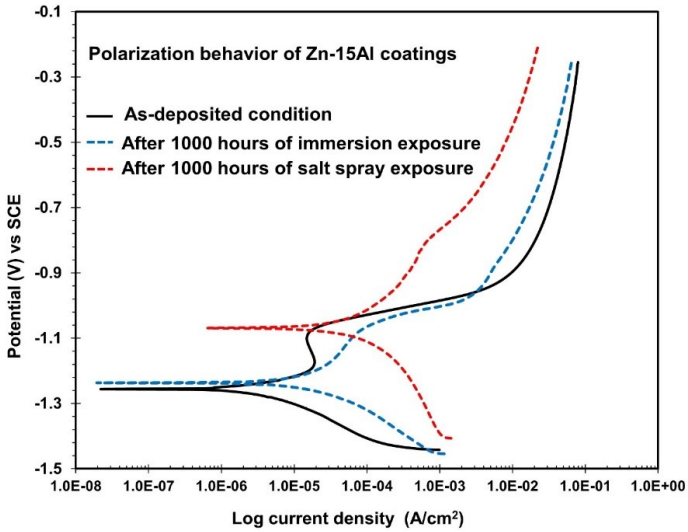

Fig. 21. Polarization curves of Zn-15Al coating in un-exposed condition and after being subjected to 1000 hours of immersion exposure and 1000 hours of salt spray exposure.

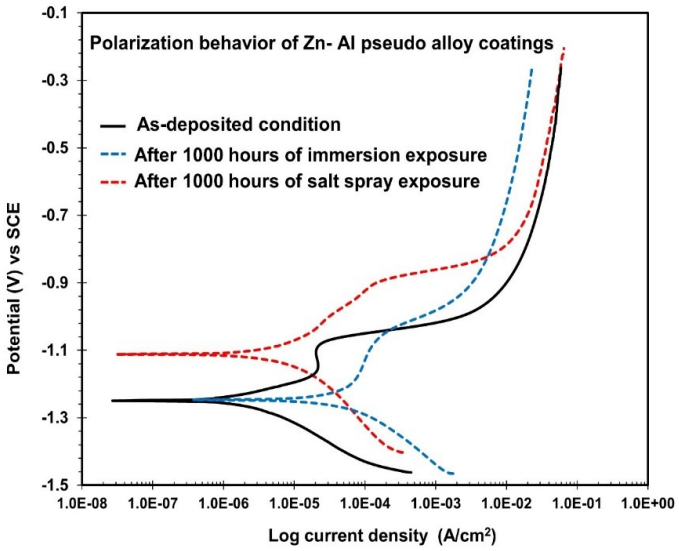

Fig. 22. Polarization curves of Zn-Al pseudo alloy coating in un-exposed condition and after being subjected to 1000 hours of immersion exposure and 1000 hours of salt spray exposure.

Table 1. Process parameters for wire-arc spraying

Spray parameter	Value, Unit
Arc voltage	32 V
Spray distance	180 mm
Current	225 Amps
Pressurized gas	Air
Inlet pressure	0.62 MPa
Substrate temperature	82 °C
Number of Passes	3

Table 2. EEC parameters that best fit the EIS data obtained from Zn-15Al and Zn-Al pseudo alloy coatings after exposure to different durations of immersion and salt spray exposures (5.0wt.% NaCl solution)

Coating	Exposure time (hours)	Rs (Ω-cm^2)	Rc (Ω-cm^2)	CPE_{po} (1×10^{-4}) (Ω^{-1} cm^{-2} s^{-n})	n_1	R_{ct} (Ω-cm^2)	CPE_{dl} (1×10^{-4}) (Ω^{-1} cm^{-2} s^{-n})	n_2
Zn-15Al (immersion)	1	4.72	12.24	31.97	0.32	806.90	93.84	0.37
	200	9.69	26.61	16.20	0.36	802.10	38.18	0.38
	400	9.50	25.62	13.41	0.45	1607.00	23.82	0.48
	600	9.16	173.50	15.72	0.52	1903.00	20.93	0.51
	800	7.69	237.40	13.20	0.59	2225.00	11.83	0.53
	1000	9.38	289.40	10.20	0.67	3804.00	6.02	0.77
Zn-15Al (salt spray)	200	15.72	28.72	27.34	0.34	820.20	29.75	0.53
	400	15.21	25.57	26.86	0.36	864.30	27.87	0.54
	600	15.86	7.98	20.27	0.48	729.90	26.08	0.61
	800	16.75	16.18	15.53	0.52	1149.00	20.88	0.68
	1000	14.87	10.78	14.62	0.55	1580.00	13.41	0.71
Zn-Al pseudo alloy (immersion)	1	14.54	34.61	12.19	0.41	494.30	115.02	0.47
	200	10.69	289.00	10.96	0.50	653.60	93.84	0.48
	400	13.69	164.60	7.64	0.52	906.80	53.01	0.50
	600	22.78	268.60	6.19	0.58	1607.08	44.64	0.52
	800	11.27	183.60	5.62	0.61	1700.00	53.12	0.53
	1000	19.13	233.50	4.39	0.63	1784.00	12.55	0.61
Zn-Al pseudo (salt spray)	200	12.56	26.28	17.70	0.43	952.70	53.27	0.53
	400	13.69	34.60	15.19	0.44	653.60	26.41	0.55
	600	16.11	171.80	7.64	0.50	1050.00	18.39	0.62
	800	19.13	164.60	5.04	0.53	1700.09	12.55	0.63
	1000	13.60	236.20	4.39	0.62	4150.07	9.53	0.71

Table 3. Electrochemical parameters obtained from Tafel extrapolation at different exposure conditions

Coating	Exposure environment and duration of exposure	E_{corr} (V) vs SCE	i_{corr} (µA/cm^2)
Zn-15Al	Un exposed	-1.26	4.53
	1000 hours of immersion	-1.24	18.49
	1000 hours of salt spray	-1.07	111.00
Zn-Al pseudo alloy	Un exposed	-1.25	1.17
	1000 hours of immersion	-1.25	29.00
	1000 hours of salt spray	-1.11	7.38

References

1. R. Singh, "Corrosion Control for Offshore Structures: Cathodic Protection and High-Efficiency Coating," Gulf Professional Publishing, 2014.
2. S. Brito, I. Bastos, and H. Costa, Corrosion Resistance and Characterization of Metallic Coatings Deposited by Thermal Spray on Carbon Steel, *Mater. Des.*, 2012, **41**, p 282–288.
3. E.E.N.E.D.E.R. Zinc and T.V.S. Acier, Field Tests on Thermally Sprayed Zinc-(Aluminium)-Coatings on Steel, *Otto-Graf-Journal*, 1999, **10**, p 60.
4. H.U. Sajid, R. Kiran, X. Qi, D.S. Bajwa, and D. Battocchi, Employing Corn Derived Products to Reduce the Corrosivity of Pavement Deicing Materials, *Construction and Building Materials*, 2020, **263**, p 120662.
5. R. Wang, L. Wang, C. He, M. Lu, and L. Sun, Studies on the Sealing Processes of Corrosion Resistant Coatings Formed on 2024 Aluminium Alloy with Tartaric-Sulfuric Anodizing, *Surf. Coat. Technol.*, 2019, **360**, p 369–375.
6. H. Huang, Z. Pan, Y. Qiu, and X. Guo, Electrochemical Corrosion Behaviour of Copper under Periodic Wet–Dry Cycle Condition, *Microelectron. Reliab.*, 2013, **53**(8), p 1149–1158.
7. H.-H. Wang and M. Du, Corrosion Behavior of a Low-Carbon Steel in Simulated Marine Splash Zone, *Acta Metall. Sin.* , 2017, **30**, p 585–593.
8. H. Katayama and S. Kuroda, Long-Term Atmospheric Corrosion Properties of Thermally Sprayed Zn, Al and Zn–Al Coatings Exposed in a Coastal Area, *Corros. Sci.*, 2013, **76**, p 35–41.
9. S. Kuroda, J. Kawakita, and M. Takemoto, An 18-Year Exposure Test of Thermal-Sprayed Zn, Al, and Zn-Al Coatings in Marine Environment, *Corrosion*, 2006, **62**(7), p 635–647.

10. Y. Li, Corrosion Behaviour of Hot Dip Zinc and Zinc-Aluminium Coatings on Steel in Seawater, *Bull. Mater. Sci.*, 2001, **24**, p 355–360.
11. Y. Xiao, X. Jiang, Y. Xiao, and L. Ma, Research on Zn-Al15 Thermal Spray Metal Coating and Its Organic Painting Composite System Protection Performance, *Procedia Engineering*, 2012, **27**, p 1644–1653.
12. A. Güleç, Ö. Cevher, A. Türk, F. Ustel, and F. Yılmaz, Accelerated Corrosion Behaviors of Zn, Al and Zn/15Al Coatings on a Steel Surface, Inst za kovinske materiale in tehnologie, 2011.
13. Q. Jiang, Q. Miao, W.-P. Liang, F. Ying, F. Tong, Y. Xu, B.-L. Ren, Z.-J. Yao, and P.-Z. Zhang, Corrosion Behavior of Arc Sprayed Al–Zn–Si–RE Coatings on Mild Steel in 3.5 Wt% NaCl Solution, *Electrochim. Acta*, 2014, **115**, p 644–656.
14. R.D. Yasoda, N. Hakim, Y. Huang, and X. Qi, Post-Fire Analysis of Thermally Sprayed Coatings: Evaluating Microstructure, Mechanical Integrity, and Corrosion Behavior, *Processes*, 2023, **11**(5), p 1490.
15. A.Q. Liu, K. Xiao, C.F. Dong, and X.G. Li, "Corrosion Behaviour of Zn-Al Pseudo-Alloy Coating on Carbon Steel in Chloride Environments," Trans Tech Publ, 2012.
16. R.D. Yasoda, Y. Huang, and X. Qi, Corrosion Performance of Wire Arc Deposited Zinc Aluminum Pseudo Alloy and Zinc 15 Aluminum Alloy Coatings on Steel in Chloride Environment, *J. Therm. Spray Technol.*, 2022, p 1–16.
17. S. Schuerz, M. Fleischanderl, G.H. Luckeneder, K. Preis, T. Haunschmied, G. Mori, and A.C. Kneissl, Corrosion Behaviour of Zn–Al–Mg Coated Steel Sheet in Sodium Chloride-Containing Environment, *Corros. Sci.*, 2009, **51**(10), p 2355–2363.

18. H. Hu, P. Zhang, D. Wei, and F. Su, Microstructure and Corrosion Behavior of Arc Sprayed Zn-XAl (X= 15, 30, 50) Alloy Coatings in NaCl Solution, *Materials Research Express*, 2019, **6**(10), p 1065f7.
19. H.-S. Lee, J.K. Singh, M.A. Ismail, C. Bhattacharya, A.H. Seikh, N. Alharthi, and R.R. Hussain, Corrosion Mechanism and Kinetics of Al-Zn Coating Deposited by Arc Thermal Spraying Process in Saline Solution at Prolong Exposure Periods, *Sci. Rep.*, 2019, **9**(1), p 1–17.
20. B.J. Usman, F. Scenini, and M. Curioni, The Effect of Exposure Conditions on Performance Evaluation of Post-Treated Anodic Oxides on an Aerospace Aluminium Alloy: Comparison between Salt Spray and Immersion Testing, *Surf. Coat. Technol.*, 2020, **399**, p 126157.
21. Y. Ma, H. Wu, X. Zhou, K. Li, Y. Liao, Z. Liang, and L. Liu, Corrosion Behavior of Anodized Al-Cu-Li Alloy: The Role of Intermetallic Particle-Introduced Film Defects, *Corros. Sci.*, 2019, **158**, p 108110.
22. A. Nishikata, Y. Ichihara, and T. Tsuru, An Application of Electrochemical Impedance Spectroscopy to Atmospheric Corrosion Study, *Corros. Sci.*, 1995, **37**(6), p 897–911.
23. D. Zhang, H. Qian, L. Wang, and X. Li, Comparison of Barrier Properties for a Superhydrophobic Epoxy Coating under Different Simulated Corrosion Environments, *Corros. Sci.*, 2016, **103**, p 230–241.
24. H.J. Martin, M.F. Horstemeyer, and P.T. Wang, Comparison of Corrosion Pitting under Immersion and Salt-Spray Environments on an as-Cast AE44 Magnesium Alloy, *Corros. Sci.*, 2010, **52**(11), p 3624–3638.

25. H.J. Martin, R.B. Alvarez, J. Danzy, M.F. Horstemeyer, and P.T. Wang, Quantification of Corrosion Pitting under Immersion and Salt Spray Environments on an As-Cast AM60 Magnesium Alloy, *Corrosion*, 2012, **68**(6), p 571–585.
26. A. B117, Standard Practice for Operating Salt Spray (Fog) Apparatus, *ASTM International (1997 Edition)*, 2011.
27. G. Astm, Standard Test Method for Conducting Potentiodynamic Polarization Resistance Measurements, *Annual Book of ASTM Standards*, 2009, **3**, p 237–239.
28. P. Marcus, "Corrosion Mechanisms in Theory and Practice," CRC press, 2011.
29. E. Calla and S.C. Modi, Long Life Corrosion Protection of Steel by Zinc-Aluminium Coating Formed by Thermal Spray Process, *Transactions-Metal Finishers Association of India*, 2001, **10**(1), p 21–26.
30. B.J. Usman, F. Scenini, and M. Curioni, Corrosion Testing of Anodized Aerospace Alloys: Comparison between Immersion and Salt Spray Testing Using Electrochemical Impedance Spectroscopy, *J. Electrochem. Soc.*, 2020, **167**(4), p 041505.
31. R. Divya Yasoda and Y. Huang, Post-Fire Mechanical Properties of Thermally Sprayed Anti-Corrosive Coatings in Oil and Gas Pipelines, *Pipelines 2022*, n.d., p 203–210.
32. D.G.A. Diaz, R.G.V. Navarro, N.O. Godoy, A.B. Pingarrón, J.R.G. Parra, J.J.O. Florez, M.T. Barragán, I.A. Moncaleano, and C.A.O. Otalora, Flame-Sprayed Zn-Al Coatings on ABS without Chemical Surface Preparation, *Mater. Lett.*, 2020, **280**, p 128574.
33. F. Zhu, D. Persson, D. Thierry, and C. Taxen, Formation of Corrosion Products on Open and Confined Zinc Surfaces Exposed to Periodic Wet/Dry Conditions, *Corrosion*, 2000, **56**(12), p 1256–1265.

34. P. Volovitch, T.N. Vu, C. Allély, A.A. Aal, and K. Ogle, Understanding Corrosion via Corrosion Product Characterization: II. Role of Alloying Elements in Improving the Corrosion Resistance of Zn–Al–Mg Coatings on Steel, *Corros. Sci.*, 2011, **53**(8), p 2437–2445.
35. R.D. Yasoda, Y. Huang, R. Kiran, and X. Qi, Post-Fire Performance of Wire-Arc-Sprayed Zn-15Al Coatings, *J. Therm. Spray Technol.*, 2023, p 1–17.
36. H.-S. Lee, J.K. Singh, and J.H. Park, Pore Blocking Characteristics of Corrosion Products Formed on Aluminum Coating Produced by Arc Thermal Metal Spray Process in 3.5wt.% NaCl Solution, *Construction and Building Materials*, 2016, **113**, p 905–916.
37. P.R. Seré, M. Zapponi, C.I. Elsner, and A.R. Di Sarli, Comparative Corrosion Behaviour of 55Aluminium–Zinc Alloy and Zinc Hot-Dip Coatings Deposited on Low Carbon Steel Substrates, *Corros. Sci.*, 1998, **40**(10), p 1711–1723.
38. A.R. Moreira, Z. Panossian, P.L. Camargo, M.F. Moreira, I.C. da Silva, and J.E.R. de Carvalho, Zn/55Al Coating Microstructure and Corrosion Mechanism, *Corros. Sci.*, 2006, **48**(3), p 564–576.
39. L.-K. Wu, J.-T. Zhang, J.-M. Hu, and J.-Q. Zhang, Improved Corrosion Performance of Electrophoretic Coatings by Silane Addition, *Corros. Sci.*, 2012, **56**, p 58–66.
40. A. Perez, A. Billard, C. Rébéré, C. Berziou, S. Touzain, and J. Creus, Influence of Metallurgical States on the Corrosion Behaviour of Al–Zn PVD Coatings in Saline Solution, *Corros. Sci.*, 2013, **74**, p 240–249.
41. V. Barranco, S. Feliu Jr, and S. Feliu, EIS Study of the Corrosion Behaviour of Zinc-Based Coatings on Steel in Quiescent 3% NaCl Solution. Part 1: Directly Exposed Coatings, *Corros. Sci.*, 2004, **46**(9), p 2203–2220.

42. Z. Wang, J. Zhang, X. Liu, J. Liu, and G. Liu, Failure Mechanism of Plasma Sprayed Tb-YSZ Coating under NaCl High-Low Temperature Cyclic Corrosion, *Surf. Coat. Technol.*, 2023, p 129244.
43. M.E. Orazem, N. Pébère, and B. Tribollet, Enhanced Graphical Representation of Electrochemical Impedance Data, *J. Electrochem. Soc.*, 2006, **153**(4), p B129.
44. G.J. Brug, A.L.G. van den Eeden, M. Sluyters-Rehbach, and J.H. Sluyters, The Analysis of Electrode Impedances Complicated by the Presence of a Constant Phase Element, *J. Electroanal. Chem. Interfacial Electrochem.*, 1984, **176**(1–2), p 275–295.
45. R.N. Amini, Z.R. Obidov, I.N. Ganiev, and R. Mohamad, Anodic Behavior of Zn-Al-Be Alloys in the NaCl Solution and the Influence of Be on Structure, *Journal of Surface Engineered Materials and Advanced Technology*, 2012, **2**(2), p 127–131.
46. Y.-Q. Wang, G. Kong, and C.-S. Che, Corrosion Behavior of Zn-Al Alloys in Saturated Ca (OH) 2 Solution, *Corros. Sci.*, 2016, **112**, p 679–686.